

Pricing Multi-Asset Options in Exponential Lévy Models

Jessica Endekovski

A dissertation submitted to the Faculty of Commerce, University of Cape Town, in partial fulfilment of the requirements for the degree of Master of Philosophy.

August 17, 2019

*MPhil in Mathematical Finance,
University of Cape Town.*



The copyright of this thesis vests in the author. No quotation from it or information derived from it is to be published without full acknowledgement of the source. The thesis is to be used for private study or non-commercial research purposes only.

Published by the University of Cape Town (UCT) in terms of the non-exclusive license granted to UCT by the author.

Declaration

I declare that this dissertation is my own, unaided work. It is being submitted for the Degree of Master of Philosophy to the University of Cape Town. It has not before been submitted for any degree or examination.

Signed by candidate

Jessica Endekovski

August 17, 2019

Abstract

This dissertation looks at implementing exponential Lévy models whereby the underlyings are driven by Lévy processes, which are able to account for stylised facts that traditional models do not, in order to price basket options more efficiently. In particular, two exponential Lévy models are implemented and tested: the multivariate Variance Gamma (VG) model and the multivariate normal inverse Gaussian (NIG) model. Both models are calibrated to real market data and then used to price basket options, where the underlyings are the constituents of the KBW Bank Index. Two pricing methods are also compared: a closed-form (analytical) approximation of the price, derived by [Linders and Stassen \(2016\)](#) and the standard Monte Carlo method. The convergence of the analytical approximation to Monte Carlo prices was found to improve as the time to maturity of the option increased. In comparison to real market data, the multivariate NIG model was able to fit the data more accurately for shorter maturities and the multivariate VG model for longer maturities. However, when looking at Monte Carlo prices, the multivariate VG model was found to outperform the results of the multivariate NIG model, as it was able to converge to Monte Carlo prices to a greater degree.

Acknowledgements

I would like to thank the University of Cape Town, and in particular, the African Institute of Financial Markets and Risk Management (AIFMRM) for providing me with the necessary resources that allowed me to complete this dissertation. I would like to thank my supervisor, Prof Peter Ouwehand, for his unwavering support and his invaluable guidance in helping me to carry out my research. I also want to thank my parents and friends for helping to motivate me during difficult times and their overall support. I also want to extend my thanks to Petro Pavlou for his interest, patience and support.

Contents

1. Introduction	1
2. Review of Literature	3
2.1 Financial Modelling	3
2.1.1 The Variance Gamma (VG) Model	4
2.1.2 Normal Inverse Gaussian (NIG) Model	5
2.2 Basket Options	6
2.3 Pricing Methods	7
2.3.1 Analytical Approximation	8
2.3.2 Monte Carlo	8
3. Lévy Processes and Asset Dynamics	9
3.1 Lévy Processes	9
3.2 The Gamma Process	10
3.3 The Variance Gamma (VG) Process	11
3.4 The Inverse Gaussian Process	13
3.5 The Normal Inverse Gaussian (NIG) Process	14
4. The Closed-Form Approximation of a Basket Option Price	17
5. Monte Carlo Simulation Study	23
5.1 Multivariate Variance Gamma	23
5.2 Multivariate Normal Inverse Gaussian	27
6. Calibration	32
6.1 Calibration Method: Non-Linear Least Squares	32
6.1.1 Variance Gamma (VG) Model	33
6.1.2 Normal Inverse Gaussian (NIG) Model	34
7. Pricing of a Basket Option	38
7.1 Comparison of Models using the Monte Carlo Method	38
7.2 Comparison of Pricing Methods	44
7.2.1 Multivariate Variance Gamma Model	44
7.2.2 Multivariate Normal Inverse Gaussian Model	50
8. Conclusion	58

Bibliography	60
A. Variance of the Price of the Basket	63

List of Figures

3.1	The gamma density for various parameters	11
3.2	The inverse Gaussian density for various parameters	14
6.1	Calibration of the VG model prices (crosses) to vanilla call options prices (circles) on 16 January 2019	36
6.2	Calibration of the NIG model prices (crosses) to vanilla call options prices (circles) on 16 January 2019	36
7.1	Monte Carlo prices of basket options for both multivariate VG (asterisks) and multivariate NIG models (circles) vs market prices (dots) on 16 January 2019, with a time to maturity of 156 days	40
7.2	Monte Carlo prices of basket options for both multivariate VG (asterisks) and multivariate NIG models (circles) vs market prices (dots) on 16 January 2019, with a time to maturity of 163 days	40
7.3	Monte Carlo prices of basket options for both multivariate VG (asterisks) and multivariate NIG models (circles) vs market prices (dots) on 16 January 2019, with a time to maturity of 349 days	41
7.4	A price comparison of Monte Carlo prices (circles), analytical approximation prices (crosses) and market prices (dots), for a call option on the KBW Bank Index on 16 January 2019 with maturity of 156 days	46
7.5	The zoomed in price comparison for the call option on the KBW Index on 16 January 2019 with maturity of 156 days (grey circle from Figure 7.4)	46
7.6	A price comparison of Monte Carlo prices (circles), analytical approximation prices (crosses) and market prices (dots), for a call option on the KBW Bank Index on 16 January 2019 with maturity of 163 days	47
7.7	The zoomed in price comparison for the call option on the KBW Index on 16 January 2019 with maturity of 163 days (grey circle from Figure 7.6)	47
7.8	A price comparison of Monte Carlo prices (circles), analytical approximation prices (crosses) and market prices (dots), for a call option on the KBW Bank Index on 16 January 2019 with maturity of 349 days	48

7.9	The zoomed in price comparison for the call option on the KBW Index on 16 January 2019 with maturity of 349 days (grey circle from Figure 7.8)	48
7.10	A price comparison of Monte Carlo prices (circles), analytical approximation prices (crosses) and market prices (dots), for a call option on the KBW Bank Index on 16 January 2019 with maturity of 156 days	53
7.11	The zoomed in price comparison for the call option on the KBW Index on 16 January 2019 with maturity of 156 days (Grey circle from Figure 7.10)	53
7.12	A price comparison of Monte Carlo prices (circles), analytical approximation prices (crosses) and market prices (dots), for a call option on the KBW Bank Index on 16 January 2019 with maturity of 163 days	54
7.13	The zoomed in price comparison for the call option on the KBW Index on 16 January 2019 with maturity of 163 days (Grey circle from Figure 7.12)	54
7.14	A price comparison of Monte Carlo prices (circles), analytical approximation prices (crosses) and market prices (dots), for a call option on the KBW Bank Index on 16 January 2019 with maturity of 349 days	55
7.15	The zoomed in price comparison for the call option on the KBW Index on 16 January 2019 with maturity of 349 days (Grey circle from Figure 7.14)	55

List of Tables

3.1	Cumulants of the VG process $(X_{VG,t}(\sigma, \nu, \mu))$	13
3.2	Cumulants of the NIG process $(X_{NIG,t}(\sigma, \nu, \mu))$	15
5.1	A comparison of the simulation results and analytical approximations for the VG model with parameters $\nu = 0.2$, weights $w = \{0.2, 0.6, 0.2\}$ and $\sigma = \{0.1, 0.1, 0.2\}$, for maturity of 1 year	25
5.2	A comparison of the simulation results and analytical approximations for the VG model with parameters $\nu = 0.2$, weights $w = \{0.2, 0.2, 0.6\}$ and $\sigma = \{0.1, 0.1, 0.2\}$, for maturity of 1 year	25
5.3	A comparison of the simulation results and analytical approximations for the VG model with parameters $\nu = 0.5$, weights $w = \{0.2, 0.6, 0.2\}$ and $\sigma = \{0.1, 0.1, 0.2\}$, for a maturity of 1 year	26
5.4	A comparison of the simulation results and analytical approximations for the VG model with parameters $\nu = 0.5$, weights $w = \{0.2, 0.2, 0.6\}$ and $\sigma = \{0.1, 0.1, 0.2\}$, for a maturity of 1 year	26
5.5	A comparison of the simulation results and analytical approximations for the VG model with parameters $\nu = 0.5$, weights $w = \{0.2, 0.2, 0.6\}$ and $\sigma = \{0.1, 0.1, 0.1\}$, for a maturity of 1 year	27
5.6	A comparison of the simulation results and analytical approximations for the NIG model with parameters $\nu = 0.2$, weights $w = \{0.2, 0.6, 0.2\}$ and $\sigma = \{0.1, 0.1, 0.2\}$, for maturity of 1 year	29
5.7	A comparison of the simulation results and analytical approximations for the NIG model with parameters $\nu = 0.2$, weights $w = \{0.2, 0.2, 0.6\}$ and $\sigma = \{0.1, 0.1, 0.2\}$, for maturity of 1 year	29
5.8	A comparison of the simulation results and analytical approximations for the NIG model with parameters $\nu = 0.5$, weights $w = \{0.2, 0.6, 0.2\}$ and $\sigma = \{0.1, 0.1, 0.2\}$, for a maturity of 1 year	30
5.9	A comparison of the simulation results and analytical approximations for the NIG model with parameters $\nu = 0.5$, weights $w = \{0.2, 0.2, 0.6\}$ and $\sigma = \{0.1, 0.1, 0.2\}$, for a maturity of 1 year	30
5.10	A comparison of the simulation results and analytical approximations for the NIG model with parameters $\nu = 0.5$, weights $w = \{0.2, 0.2, 0.6\}$ and $\sigma = \{0.1, 0.1, 0.1\}$, for a maturity of 1 year	31
6.1	Calibrated parameters of the Lévy triplet for the VG model and the resulting minimised RMSE	34

6.2	Calibrated parameters of the Lévy triplet for the NIG model and the resulting minimised RMSE	35
7.1	A Summary of the RMSE for basket options with various maturities and priced using the multivariate VG and multivariate NIG models .	39
7.2	Monte Carlo price using the multivariate VG model vs the market price for basket options priced on 16 Januray 2019 for various maturities	42
7.3	Monte Carlo price using the multivariate NIG model vs the market price for basket options priced on 16 Januray 2019 for various maturities	43
7.4	A Summary of the RMSE and absolute errors between the Monte Carlo and analytical approximation prices for basket options with various maturities, when implemented for the multivariate VG model	45
7.5	The analytical approximation prices vs the Monte Carlo prices for a basket call option on 16 January 2019	49
7.6	A Summary of the RMSE and absolute errors between the Monte Carlo and analytical approximation prices for basket options with various maturities, when implemented for the multivariate NIG model	51
7.7	A comparison of the RMSE values between the Monte Carlo and analytical approximation prices for basket options with various maturities, for the multivariate VG model versus the multivariate NIG model	52
7.8	The analytical approximation prices vs the Monte Carlo prices for a basket call option on 16 January 2019	56
7.9	A comparison of the efficiency of the pricing methods, in terms of the run-time of the code	57

Chapter 1

Introduction

The interest in multi-asset products is growing as they provide a way of increasing diversification and thus reducing risk. Basket options in particular have the advantage of allowing traders to personalise and have more control over their choice of investment, by allowing them to choose specific underlyings to make up the basket. This growing interest has led to a search for financial models that are able to fit real market data more accurately than the traditional models, so that they may be used to price various products more efficiently. These traditional models have been based on the normal distribution and Gaussian dependence, which, as a result, has led to some inefficiencies in financial modelling ([Papapantoleon, 2008](#)). These classical models do not account for tail dependence and also fail to incorporate share price jumps experienced in the market.

Lévy processes have gained significant popularity amongst practitioners and academics alike, due to their marginal infinite divisibility and the flexibility of their distribution. However, the applications of Lévy processes are not restricted to mathematical finance alone. In reality, the application stretches to the scientific fields where they are used to study laser cooling and turbulence; to actuarial science where they are used to calculate insurance and re-insurance risk and even in engineering for the study of networks ([Papapantoleon, 2008](#)). In mathematical finance, the observed behaviour of asset prices often includes jumps or spikes, which practitioners need to consider when managing risk. Asset returns often have an empirical distribution that deviates from normality ([Sheikh and Qiao, 2010](#)), specifically in terms of stylised facts such as skewness, kurtosis and fat tails. This reality has contributed to the popularity of Lévy processes as they are able to describe observed reality in financial markets more accurately than Geometric Brownian motion.

This dissertation will explore the use of models based on subordinated Brownian motion, i.e. where the underlyings are driven by Lévy processes. In particular, the multivariate Variance Gamma (VG) model and the multivariate normal inverse Gaussian (NIG) model will be implemented and tested. These models will

be used to price multi-asset options - in particular, basket options - using both the approximate closed-form expression derived by [Linders and Stassen \(2016\)](#) and the conventional Monte Carlo method.

This dissertation is structured as follows: in Chapter 2, a review of literature is presented, where previous research that has been conducted using the multivariate VG model as well as the multivariate NIG model is discussed. The two pricing methods to be used in this dissertation are also explored (i.e. Monte Carlo and an analytical approximation). Chapter 3 provides a more technical background to this research and in particular, delves into Lévy processes in more detail. The mathematical aspects relating to the Variance Gamma and normal inverse Gaussian processes are also covered. Chapter 4 presents the derivation of the analytical approximation and Chapter 5 details a Monte Carlo simulation study on this analytical approximation. In this study, both the multivariate VG and NIG models are used to test the analytical approximation against Monte Carlo pricing. In Chapter 6, the focus is on calibrating the models to real market data. Parameters for each model are estimated using vanilla options data on each constituent of the KBW Bank Index using a nonlinear least squares method. Chapter 7 is split into two main sections: the first section uses the Monte Carlo pricing method along with the newly calibrated models to price basket options, and then compares these prices to market prices. The second section then draws a comparison of the Monte Carlo pricing method and the analytical approximation, for both models. Finally, in Chapter 8, conclusions are drawn pertaining to the entire dissertation.

Chapter 2

Review of Literature

2.1 Financial Modelling

Historically, Brownian motion was the industry standard for modelling asset returns in continuous time, but since then research has suggested that standard Brownian motion does not sufficiently take note of different stylised facts of asset returns - such as skewness and kurtosis (Papapantoleon, 2008). Geometric Brownian motion is a continuous-time process which means it does not account for any price jumps that may occur. This is where the introduction of models that are able to incorporate jumps become valuable to the financial world. Two such model classes exist - those with a finite number of jumps, termed "jump-diffusion" models and those with an infinite number of jumps, termed "infinite activity" models (Cont and Tankov, 2003). Carr and Wu (2004) are of the opinion that the price of assets constantly fluctuates and thus exhibits many small jumps, making the infinite activity models the better choice for describing the price process. For this dissertation, the use of models from this class is explored. In particular, the focus is on Lévy models, which are based on subordinated Brownian motion and the extension of these models to multi-dimensions is performed, for the purpose of pricing basket options. The underlyings of the basket (i.e. stocks in this case) are driven by Lévy processes. The appeal of the application of the Lévy process lies in the flexibility of its distribution. The distribution has fatter tails, allowing for the occurrence of extreme events to be modelled with higher probabilities. Lévy processes also take into account excess kurtosis and skewness, that normally-distributed processes do not (Linders and Stassen, 2016). The extension of Lévy models to higher dimensions is achieved by using a subordinator to time-change the multidimensional Brownian motions (Cont and Tankov, 2003). Lévy processes and subordinators are defined mathematically in Chapter 3.

The focus of this dissertation will be on two exponential Lévy models: the Variance Gamma (VG) model, where the subordinator has a gamma distribution, and

the Normal Inverse Gaussian (NIG) model, where the subordinator has an inverse Gaussian distribution.

2.1.1 The Variance Gamma (VG) Model

[Madan and Seneta \(1987\)](#) introduced the VG process and used this to model stock returns. Since then, the VG process has successfully been implemented for modelling both interest rates and equity ([Madan and Seneta, 1990](#)), ([Schoutens, 2003](#)), ([Rathgeber et al., 2016](#)). The VG model has also been used to model various option types, including the research done by [Luciano and Schoutens \(2006\)](#), [Avramidis and L'Ecuyer \(2006\)](#), [Linders and Stassen \(2016\)](#) to price basket options, [Ballotta and Bonfiglioli \(2016\)](#) to price spread options and [Hirsa and Madan \(2004\)](#) to price American options.

[Madan et al. \(1998\)](#) compared the VG model to the Black-Scholes model by running orthogonality tests. The purpose of these tests was to assess the quality of the pricing that was performed by the models by testing the predictability of the pricing errors and whether these errors possessed any consistent pattern (this was seen as unfavourable). [Madan et al. \(1998\)](#) concluded that the VG model outperformed the Black-Scholes model.

In 2006, [Luciano and Schoutens \(2006\)](#) calibrated and used the multivariate VG model to price rainbow options. The authors found that calibration of the model was fast and it yielded good results in terms of matching both equity and credit derivative data. According to [Luciano and Schoutens \(2006\)](#), the calibration of this model was easy to simulate as it could be done using univariate derivatives products. This is of particular value for this dissertation as basket option prices are generally not observable in the market and thus the ability to use univariate derivatives to calibrate the model would offer a faster and effective solution for the calibration procedure. Making use of univariate derivatives products for calibration is possible, owing to the fact that the joint and marginal distributions of this model depend on the same parameters at any fixed time point, according to the authors.

Authors [Semeraro \(2008\)](#), [Ballotta and Bonfiglioli \(2016\)](#) and [Luciano et al. \(2016\)](#) investigate the dependence structure of multivariate Lévy processes, and VG processes in particular. In the paper by [Semeraro \(2008\)](#), the focus is placed on modelling the dependence between asset returns and the implementation of various Lévy models as the marginal distribution of returns. The method followed in this paper allows for the calibration process to become more tractable, as it is broken down into two steps: firstly, calibrating marginal returns distributions and secondly, calibrating the dependence structure. The authors conclude that these models outperform Gaussian models.

In [Linders and Stassen \(2016\)](#) and [Luciano and Schoutens \(2006\)](#), both papers suggest the use of a multivariate Variance Gamma model which has the advantage of possessing both the strengths of the univariate VG process and includes a non-Gaussian dependence structure. [Linders and Stassen \(2016\)](#) price basket options using the multivariate VG model where the individual stock prices are dependent through a common time change. The basket was constructed by a weighted sum of correlated Brownian motions which was conditioned on the time change. The derived closed-form approximation given by [Linders and Stassen \(2016\)](#) is to be implemented and analysed in this dissertation, and is given by:

$$\bar{C}[K] = \int_0^{+\infty} \bar{C}[K; y] f_G(y) dy, \quad (2.1)$$

where f_G is the density of the Gamma subordinator.

The conditional approximation $\bar{C}[K; y]$ is broken down into conditional upper and lower bounds:

$$\bar{C}[K; y] = e^{-rT} \left(z_y \mathbb{E} \left[(S_{\text{basket}}^{\text{low}} - K)^+ \right] + (1 - z_y) \mathbb{E} \left[(S_{\text{basket}}^{\text{up}} - K)^+ \right] \right). \quad (2.2)$$

Here, K is the strike, r is the risk-free rate, G is the Gamma subordinator, S is the price of the underlying, *low* and *up* denote 'lower' and 'upper' and z_y is the weighting factor for the bounds. More on this derivation is to follow in Chapter 4.

[Linders and Stassen \(2016\)](#) observed that the VG model was a close match with observed index options and was a good estimate for implied correlation.

2.1.2 Normal Inverse Gaussian (NIG) Model

The normal inverse Gaussian distribution was first published in the field of mathematical finance by [Barndorff-Nielsen \(1997\)](#). This author was also the person who discovered the generalised hyperbolic distribution, of which the NIG distribution is sub-categorised. [Barndorff-Nielsen \(1997\)](#) describes the NIG distribution as a "variance-mean mixture distribution", where it is based on the normal distribution and "mixed" by an inverse Gaussian distribution. He also concludes that by using the NIG process, one is able to construct stochastic processes that are able to capture key stylised facts (such as excess kurtosis and skewness) more accurately than Gaussian processes. Since 1997, there have been various research studies performed using the NIG process. The NIG model has been studied by [Kalemanova et al. \(2007\)](#) to price synthetic CDOs, by [Benth et al. \(2006\)](#) for pricing vanilla and Asian options and by [Sæbø \(2009\)](#) for pricing lookback options.

[Benth and Šaltytė-Benth \(2004\)](#) use the normal inverse Gaussian distribution in the modelling of spot prices related to the oil and gas markets and then later priced

forwards and options. They conclude that the NIG distribution provides a better fit to this data than that of the Gaussian model.

Wu et al. (2009) use the multivariate NIG process to derive an approximation of both an arithmetic and a geometric basket option price. The authors were able to derive an exact analytical solution for the price of a geometric basket option, but were only able to derive an approximation for the price of an arithmetic basket option. Wu et al. (2009) also performed a Monte Carlo empirical study on the NIG model and the approximate prices (for both types of basket options) and found it to match the Monte Carlo prices within 1% error, indicating the accuracy of the model prices when compared to the "true" (Monte Carlo) prices.

The research on dependence structures of multivariate Lévy processes that were discussed by Ballotta and Bonfiglioli (2016), Semeraro (2008) and Luciano et al. (2016) also can be applied to NIG models. It also suggested that the calibration method of first calibrating marginal parameters and then calibrating the dependence structure can be implemented for NIG models as well.

According to Linders and Stassen (2016), the approximation for a basket option that is derived in their paper can also be applied to other subordinators outside of the gamma subordinator of the VG model. Thus, we are able to use the same approximation of the basket price, but slightly altering it to cater for the NIG model instead of the VG model. This leads to the closed-form approximation price in this paper to be re-written as:

$$\bar{C}[K] = \int_0^{+\infty} \bar{C}[K; y] f_I(y) dy, \quad (2.3)$$

where f_I is now the density of the inverse Gaussian subordinator.

The conditional approximation $\bar{C}[K; y]$ is still broken down into conditional upper and lower bounds, as seen in Equation 2.2.

2.2 Basket Options

A basket option is an exotic option that has a payoff dependent on the weighted sum of different underlying assets that have been grouped together (Cont and Tankov, 2003). This is where the holder of the option has the right, but not the obligation, to purchase or sell the basket of underlyings at a given strike price, at the expiry date.

The basket (S_b) can be written as follows:

$$S_b(t) = \sum_{i=1}^n w_i X_i(t),$$

where w_i and $X_i(t)$ are the weight and price for $i = 1$ to n underlyings at time t , respectively.

Two of the simplest examples are a call and a put on the portfolio of assets. The payoffs of each of these options are given as follows:

For a call option on the basket:

$$\left(\sum_{i=1}^n w_i X_i(T) - K \right)^+$$

For a put option on the basket:

$$\left(K - \sum_{i=1}^n w_i X_i(T) \right)^+$$

where K is the strike and T is the expiry.

The focus of this dissertation will be to price an index option, which is essentially a basket option, where the basket consists of the constituents of the index. The underlyings in an index can be weighted by different methods, for example, by price or market capitalisation. Options on the KBW Bank Index will be priced. This index was chosen because its historical options data (that is used for calibration and pricing) is observable in the market and is easily obtainable using the Bloomberg terminal.

The KBW Bank Index was developed by Keefe, Bruyette and Woods, an investment banking firm that specialises exclusively in the financial sector. The index has 24 large-cap banking stocks as constituents and was historically viewed as the benchmark of the banking sector in the stock market (Chen, 2018). This index is modified-capitalisation weighted, as is detailed in Chapter 7.

2.3 Pricing Methods

Two pricing methods will be carried out and compared, namely: an analytical approximation that was derived by Linders and Stassen (2016) and the well-known Monte Carlo method. The two methods will be compared in terms of accuracy of results and coding run-time efficiency.

2.3.1 Analytical Approximation

[Linders and Stassen \(2016\)](#) derived a closed-form expression that approximates the price of a basket option as a linear combination of Black-Scholes prices. This was achieved by approximating convex upper and lower bounds and by modelling the stock prices with a multivariate VG model and making them dependent through a common time-changed Brownian motion. This derivation will be discussed in greater detail in Chapter 4. The approximation will also be adjusted to make use of a multivariate NIG model instead of the multivariate VG model.

2.3.2 Monte Carlo

The Monte Carlo method is based upon risk-neutral valuation, i.e. the price of the option is equal to the discounted expected value. This method involves the simulation of a number of paths for the price of the underlying. Once these paths have been simulated, the price of the option is determined by calculating the various payoffs, which are then averaged and discounted back ([Boyle et al., 1997](#)). The popularity of this method has been due to its ability to price options that contain some level of uncertainty and complex features.

Chapter 3

Lévy Processes and Asset Dynamics

3.1 Lévy Processes

Lévy processes are widely used in various fields other than mathematical finance and thus have been well-researched. There is comprehensive literature available on Lévy processes and their applications and can be found in [Barndorff-Nielsen et al. \(2012\)](#), [Kyprianou \(2006\)](#), [Cont and Tankov \(2003\)](#), [Schoutens \(2002\)](#), [Sato \(1999\)](#) and [Kyprianou et al. \(2006\)](#).

A Lévy process, first introduced by French mathematician Paul Lévy in the 1930s, is a càdlàg stochastic process with the properties described in Definition 3.1.

Definition 3.1. (Lévy Process)

A Lévy process, $(L_t)_{t \geq 0}$, is a càdlàg stochastic process that starts at zero ($L_0 = 0$), with values in \mathbb{R}^d , conditional on it possessing the following key properties:

- *Independent increments:* the increments $L_{t_n} - L_{t_{n-1}}$ are seen as independent random variables, for non-overlapping time sequences.
- *Stationary increments:* the probability distribution of the interval $L_{t_n+h} - L_{t_n}$ does not depend on t_n itself, but on the length of the interval of time, h .
- *Stochastic continuity:* $\forall \epsilon > 0, \lim_{h \rightarrow 0} \mathbb{P}(|L_{t+h} - L_t| \geq \epsilon) = 0$.

It must be noted that the property of stochastic continuity does not suggest that sample paths must be continuous, as is seen by the Poisson process, a well-known Lévy process that has discontinuous paths ([Cont and Tankov, 2003](#)).

Definition 3.2. (Infinite divisibility)

Consider P , a probability distribution that exists on \mathbb{R}^d . If for any integer $n \geq 2$, there exists

n i.i.d. random variables X_1, X_2, \dots, X_n , whose sum $X_1 + X_2 + \dots + X_n$ has distribution P , then the distribution P is infinitely divisible.

The following proposition is given by [Cont and Tankov \(2003\)](#):

Proposition 3.3. (Characteristic function of a Lévy process)

The Lévy process $(L_t)_{t \geq 0}$ that exists on \mathbb{R}^d , has the following characteristic function:

$$\mathbb{E}[e^{i\theta L_t}] = e^{t\psi(\theta)}, \theta \in \mathbb{R}^d, \quad (3.1)$$

where $\psi : \mathbb{R}^d \rightarrow \mathbb{R}$ is a continuous function that is termed the characteristic exponent of L_t .

The following theorem is given by [Cont and Tankov \(2003\)](#):

Theorem 3.4. (The Lévy-Khinchin Formula)

Consider a Lévy process $(L_t)_{t \geq 0}$, with a Lévy triplet (σ, ν, μ) that exists on \mathbb{R}^d .

Then, referring to Equation 3.1, note the characteristic exponent $\psi(\theta)$, is:

$$\psi(\theta) = -\frac{1}{2}\theta \cdot \sigma \theta + i\mu \cdot \theta + \int_{\mathbb{R}^d} \left(e^{i\theta \cdot x} - 1 - i\theta \cdot x I_{|x| \leq 1} \right) \nu dx.$$

The characteristic function is the Fourier transform of the density. However, the density of many Lévy processes is either computationally expensive, or it is unknown in closed form, but by Lévy-Khinchin, the characteristic function is often known and relatively simple. This allows for pricing by Fourier methods.

Theorem 3.5. (Subordinator)

If L_t is a Lévy process and S is a subordinator, then X_{S_t} is a Lévy process as well.

A subordinator then classified as a subclass of Lévy processes. Specifically, it is an a.s. increasing Lévy process that can be used as a time change for other Lévy processes.

3.2 The Gamma Process

The Gamma process, which we can denote as $G(t) = \{G(t), t \geq 0\}$, is defined by [Luciano and Schoutens \(2006\)](#) as an increasing Lévy process, i.e. a subordinator, which follows a Gamma distribution. A Gamma distribution is a continuous probability distribution that is reliant on two parameters.

The following information regarding the Gamma process was obtained from [Luciano and Schoutens \(2006\)](#).

The random variable X_t that has a $\text{Gamma}(\alpha, \beta)$ distribution has the following density function:

$$f_{X_t}(x; \alpha, \beta) = \frac{\beta^\alpha}{\Gamma(\alpha)} x^{\alpha-1} e^{(-x\beta)}, x \geq 0, \quad (3.2)$$

where the shape and rate parameters are $\alpha \geq 0$ and $\beta \geq 0$, respectively.

The gamma density shown for various parameters in Figure 3.1 illustrates its semi-heavy right-tailed shape.

The characteristic function of the random variable X_t with Gamma(α , β) distribution is given by:

$$\phi_{X_t}(u; \alpha, \beta) = \left(1 - \frac{iu}{\beta}\right)^{-\alpha}. \quad (3.3)$$

According to the theory on Lévy processes that is presented in [Sato \(1999\)](#) and [Schoutens \(2003\)](#), if we consider increments that run over intervals of length t , then the distribution of these increments is Gamma(αt , β).

From this, and also by following the procedures of [Linders and Stassen \(2016\)](#) and [Luciano and Schoutens \(2006\)](#), throughout this dissertation, it is assumed that the Gamma process follows a Gamma distribution with parameters αt and β . These parameters are chosen for normalization reasons, as this allows $\mathbb{E}[G(t)] = t$. Note the following notation: $\nu = \frac{1}{\alpha}$ and $\alpha = \beta$.

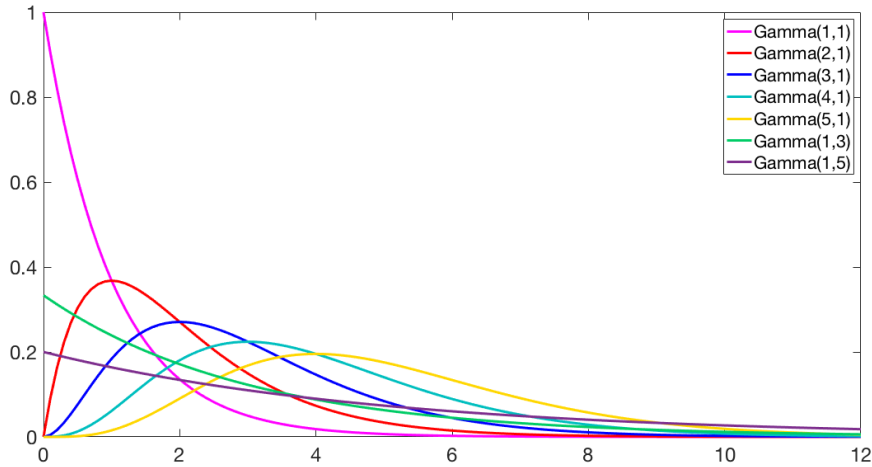


Fig. 3.1: The gamma density for various parameters

3.3 The Variance Gamma (VG) Process

The Variance Gamma process is a Lévy process, thus it possesses all the properties of a Lévy process, i.e. stationary and independent increments and stochastic continuity (See section 3.1 for reference). According to [Luciano and Schoutens](#)

(2006), the VG model is based on independent Brownian motion and uses a technique called stochastic time-changing to incorporate skewness, kurtosis, stochastic volatility and non-Gaussian dependence.

To show this, we suppose $B_t(\mu, \sigma)$ is a Brownian motion with drift μ and volatility σ . Then its dynamics are given by:

$$dB_t = \mu dt + \sigma dW_t,$$

where W_t denotes a standard Brownian motion.

Let $X(t) = \{X_{VG}(t), t \geq 0\}$ denote the VG process, we can then show the VG process in terms of Brownian motion B_t and the Gamma process G_t given in section 3.2:

$$\begin{aligned} X_t(\sigma, \nu, \mu) &= B_{G(t)}(\mu, \sigma) \\ &= \mu G(t) + \sigma W(G(t)). \end{aligned}$$

The VG process has three parameters: μ and σ , the drift and volatility of Brownian motion and ν , the variance of the subordinator.

Cont and Tankov (2003) gives the probability density of VG as:

$$f_{X_t}(x) = C|x|^{\frac{t}{\nu}-0.5} e^{Ax} K_{\frac{t}{\nu}-0.5}(B|x|), \quad (3.4)$$

where:

$$C = \sqrt{\frac{\sigma^2 \nu}{2\pi}} \frac{(\mu^2 \nu + 2\sigma^2)^{\frac{1}{4} - \frac{\mu}{2\nu}}}{\Gamma(\frac{t}{\nu})},$$

$$A = \frac{\mu}{\sigma^2},$$

$$B = \frac{\sqrt{\mu^2 + \frac{\sigma^2}{\nu}}}{\sigma^2}$$

and K_n is a modified Bessel function of the second kind.

The characteristic function of the VG process is given as:

$$\phi_{X_t}(\theta) = \left(\frac{1}{1 - i\theta\mu\nu + \frac{1}{2}\theta^2\sigma^2\nu} \right)^{\frac{t}{\nu}}. \quad (3.5)$$

The cumulants of the VG process are given in Table 3.1, as per [Cont and Tankov \(2003\)](#).

Tab. 3.1: Cumulants of the VG process ($X_{VG,t}(\sigma, \nu, \mu)$)

Mean	μt
Variance	$\sigma^2 t + \mu^2 \nu t$
Skewness	$3\sigma^2 \mu \nu t + 2\mu^3 \nu^2 t$
Kurtosis	$3\sigma^4 \nu t + 6\mu^4 \nu^3 t + 12\sigma^2 \mu^2 \nu^2 t$

We can extend the univariate Variance Gamma process to the multivariate version using the form of the multivariate Variance Gamma vector X given by [Semeraro \(2008\)](#), and below we show the form of the i^{th} component of vector X :

$$X_i(\sigma_i, \nu, \mu_i) = \mu_i G_i + \sigma_i \sqrt{G_i} W_i, \quad (3.6)$$

where W_i is a standard normal random number and G_i is a Gamma random number, independent of W_i . It must be noted that while there are n means and volatilities (μ_i, σ_i , since $i = 1, 2, \dots, n$), there is only one constant subordinator variance ν , which is the same for each i^{th} component of X .

3.4 The Inverse Gaussian Process

In the case of the NIG model, the subordinator is an increasing Lévy process that follows an inverse Gaussian distribution. The inverse Gaussian process, (the subordinator), is denoted by $I(t) = \{I(t), t \geq 0\}$. An inverse Gaussian distribution is also a continuous probability distribution, reliant on two parameters: the mean parameter μ and shape parameter λ .

[Tweedie \(1941\)](#) and [Folks and Chhikara \(1978\)](#) give the density function of a random variable X_t , that is distributed as inverse Gaussian, as the following:

$$f_{X_t}(x; \mu, \lambda) = \left(\frac{\lambda}{2\pi x^3} \right)^{\frac{1}{2}} e^{-\frac{\lambda(x-\mu)^2}{2\mu^2 x}}, x \geq 0, \quad (3.7)$$

where the mean and shape parameters are $\mu \geq 0$ and $\lambda \geq 0$, respectively.

Figure 3.2 illustrates how the shape of the density function for inverse Gaussian of various parameters is also semi-heavy right-tailed.

The characteristic function of the random variable X_t with a distribution that is Inverse Gaussian(μ, λ) is given by [Folks and Chhikara \(1978\)](#) as:

$$\phi_{X_t}(u; \mu, \lambda) = e^{\frac{\lambda}{\mu} \left[1 - \sqrt{1 - \frac{2i\mu^2 u}{\lambda}} \right]}. \quad (3.8)$$

Note the following notation: $\nu = \frac{1}{\lambda}$, where ν is the variance of the subordinator and also note that the value of $\mu = 1$.

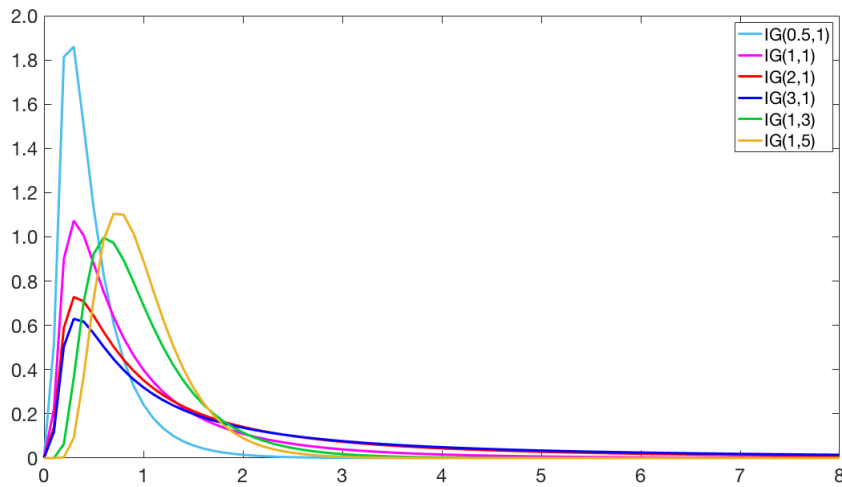


Fig. 3.2: The inverse Gaussian density for various parameters

3.5 The Normal Inverse Gaussian (NIG) Process

The normal inverse Gaussian process is also a Lévy process, thus it too possesses the properties of a Lévy process, i.e. stationary and independent increments and also stochastic continuity (See section 3.1 for reference). According to [Cont and Tankov \(2003\)](#), the normal inverse Gaussian process can be obtained by using an inverse Gaussian subordinator to subordinate a Brownian motion (stochastic time-changing). The method for illustrating stochastic time-change was given in section 3.3, but will be altered here to incorporate an inverse Gaussian subordinator instead of the Gamma subordinator used in the VG process.

We suppose again that $B_t(\mu, \sigma)$ is a Brownian motion with drift μ and volatility σ . Then its dynamics are given by:

$$dB_t = \mu dt + \sigma dW_t,$$

where W_t denotes a standard Brownian motion.

Let $X(t) = \{X_{NIG}(t), t \geq 0\}$ denote the NIG process, we can then show the NIG process in terms of Brownian motion B_t and the inverse Gaussian process I_t of section 3.4:

$$\begin{aligned} X_t(\sigma, \nu, \mu) &= B_{I(t)}(\mu, \sigma) \\ &= \mu I(t) + \sigma W(I(t)). \end{aligned}$$

The NIG process has three parameters: μ and σ , the drift and volatility of Brownian motion and ν , the variance of the subordinator.

[Cont and Tankov \(2003\)](#) give the probability density of NIG as:

$$f_{X_t}(x) = C e^{-Ax \frac{K_1\left(B\sqrt{x^2 + \frac{t^2\sigma^2}{\nu}}\right)}{\sqrt{x^2 + \frac{t^2\sigma^2}{\nu}}}}, \quad (3.9)$$

where:

$$\begin{aligned} C &= \frac{t}{\pi} e^{t/\nu} \sqrt{\frac{\mu^2}{\nu\sigma^2} + \frac{1}{\nu^2}}, \\ A &= \frac{\mu}{\sigma^2}, \end{aligned}$$

$$B = \frac{\sqrt{\mu^2 + \sigma^2/\nu}}{\sigma^2},$$

and K_n is a modified Bessel function of the second kind.

The characteristic function of the NIG process is given as:

$$\phi_{X_t}(\theta) = e^{\left(\nu - \sigma \sqrt{\frac{\nu^2}{\sigma^2} + \frac{\mu^2}{\sigma^4} - \left(\frac{\mu}{\sigma^2} + i\theta\right)^2}\right)T}. \quad (3.10)$$

The cumulants of the NIG process are given in Table 3.2, as per [Cont and Tankov \(2003\)](#).

Tab. 3.2: Cumulants of the NIG process ($X_{NIG,t}(\sigma, \nu, \mu)$)

Mean	μt
Variance	$\sigma^2 t + \mu^2 \nu t$
Skewness	$3\sigma^2 \mu \nu t + 3\mu^3 \nu^2 t$
Kurtosis	$3\sigma^4 \nu t + 15\mu^4 \nu^3 t + 18\sigma^2 \mu^2 \nu^2$

Wu et al. (2009) give the multivariate normal inverse Gaussian process as a vector (X) and we show the form of the i^{th} component of vector X as:

$$X_i(\sigma_i, \nu, \mu_i) = \mu_i I_i + \sigma_i \sqrt{I_i} W_i, \quad (3.11)$$

where W_i is a standard normal random number and I_i is a random number has an inverse Gaussian distribution, and is independent of W_i . It must be noted that while there are n means and volatilities $(\mu_i, \sigma_i, \text{ since } i = 1, 2, \dots, n)$, there is only one constant subordinator variance ν , which is the same for each i^{th} component of X .

Chapter 4

The Closed-Form Approximation of a Basket Option Price

This chapter details the derivation of the closed-form approximation price of a basket option given by [Linders and Stassen \(2016\)](#), where the constituents of the basket are stocks.

The approximation is derived using a financial model that is based on the multivariate Variance Gamma (VG) model proposed by [Luciano and Schoutens \(2006\)](#). However, in this chapter we consider the derivation for a general case of subordinator. We introduce the following notation: r is the deterministic risk-free rate and the process $\{H(t)|t \geq 0\}$ is an increasing Lévy process which starts at zero (the subordinator). For the multivariate VG model, the subordinator is Gamma-distributed, i.e. $H(t) = G(t)$ and for the multivariate NIG model, the subordinator is inverse Gaussian-distributed, i.e. $H(t) = I(t)$. $B(t)$ is a standard Brownian motion process that is independent of the process $H(t)$.

We consider the stock price at time t , denoted by $S_i(t)$, and has risk-neutral dynamics which are given as follows:

$$S_i(t) = S_i(0)e^{\{(r-q_i+\omega_i)t+\mu_i H(t)+\sigma_i B_i(H(t))\}}, \quad \text{for } i = 1, 2, \dots, n \quad (4.1)$$

where ω_i , the "martingale correction" term, is

$$\omega_i = \frac{1}{\nu} \log \left(1 - \frac{1}{2} \sigma_i^2 \nu \right) \text{ for VG,} \quad (4.2)$$

and

$$\omega_i = -\frac{1}{T} \log \left(e^{(\nu - \sigma_i \sqrt{\frac{\nu^2 + \frac{\mu_i^2}{\sigma_i^4} - (\frac{\mu_i}{\sigma_i^2} + 1)^2})T} \right) \text{ for NIG,} \quad (4.3)$$

and q_i is the rate at which dividends are paid continuously, for a given stock i .

It must be noted that while each stock i has its own μ_i , σ_i and ω_i , all stocks have the same subordinator.

We consider a basket with n underlying stocks as constituents, that possess these risk-neutral dynamics. This allows for the stock price dynamics to be expressed as exponentials of the respective process, i.e. Variance Gamma (VG) or normal inverse Gaussian (NIG), which are both exponential Lévy processes. The price of the basket (denoted as $S_b(t)$) can be written as a linear combination of the stocks and their respective weighting:

$$S_b(t) = w_1 S_1(t) + w_2 S_2(t) + \dots + w_n S_n(t). \quad (4.4)$$

The distribution of the basket price is written as follows:

$$S_b(T) \sim \sum_{i=1}^n w_i S_i(0) e^{(r - q_i + \omega_i)T + \mu_i H(T) + \sigma_i \sqrt{H(T)} Z_i}, \quad (4.5)$$

where $Z_i(1) \sim N(0, 1)$.

From here on, we will drop the explicit dependence of H on T .

The elements of S_b have a distribution that is log-normal, conditional on the subordinator H :

$$\ln \frac{S_i}{S_i(0)} \sim N((r - q_i + \omega_i)T + \mu_i H, \sigma_i^2 H).$$

From the distribution given in Equation 4.5, we denote the conditional random variable as $S_b|H$. This variable is a sum of n dependent random variables that are lognormally distributed and weighted by a factor w_i . They also have pairwise correlations, denoted as $\rho_{i,j}$.

The basket option price $C[K]$ is then derived using the tower property:

$$C[K] = \int_0^{+\infty} e^{-rT} \mathbb{E}[(S - K)_+ | H = y] f_H(y) dy, \quad (4.6)$$

where $f_H(y)$ is the density function of the subordinator H , given by Equation 3.2 for $G(t)$ and Equation 3.7 for $I(t)$.

In order to find an approximation for the basket option price ($C[K]$) given in Equation 4.6, first we must approximate the integrand $e^{-rT} \mathbb{E}[(S - K)_+ | H = y]$ through use of the theory of comonotonicity and the decomposition formula, detailed in theorems 4.2 and 4.3 below.

Then, we approximate the integral $\int_0^{+\infty} e^{-rT} \mathbb{E}[(S - K)_+ | H = y] f_H(y) dy$ by using a method of quadrature to discretise the integral.

Comonotonicity

The following definitions were sourced from [Kaas et al. \(2008\)](#) and will be applicable to the derivation in Chapter 4.

Definition 4.1. (Convex Order)

Consider two random variables, X and Y . X is less than Y in convex order, written as $X \leq_{cx} Y$, if the following conditions hold true for every $k \in \mathbb{R}$:

$$\begin{aligned}\mathbb{E}[(X - k)_+] &\leq \mathbb{E}[(Y - k)_+], \text{ and} \\ \mathbb{E}[(k - X)_+] &\leq \mathbb{E}[(k - Y)_+].\end{aligned}$$

Consider a random vector (X_1, \dots, X_n) . If it has a comonotonic distribution, then it is deemed a comonotonic random vector. We see this in the following theorem:

Theorem 4.2. (Comonotonic Joint Distribution)

Consider a random vector $\bar{X} =: (X_1, \dots, X_n)$, the comonotone equivalent is then defined as follows:

$$\bar{Y} := (Y_1, \dots, Y_n) = \left(F_{X_1}^{-1}(U), \dots, F_{X_n}^{-1}(U) \right), \quad (4.7)$$

where U is a uniform random number with $U \sim (0, 1)$ and the comonotone equivalent holds the following properties:

- \bar{Y} and \bar{X} have the same marginals, i.e. $Y_i \sim X_i \forall i$.
- it has a comonotonic distribution.
- Its joint CDF is equivalent to the Fréchet/Höfding upper bound:

$$Pr[Y_1 \leq y_1, \dots, Y_n \leq y_n] = \min_{j=1, \dots, n} Pr[X_j \leq y_j]. \quad (4.8)$$

The decomposition formula was extracted from [Linders and Stassen \(2016\)](#).

Theorem 4.3. (Decomposition Formula)

Consider S to be a weighted sum of the comonotonic random variables (X_1, X_2, \dots, X_n) . Assume the continuous CDF F_s is strictly increasing on $[0, +\infty)$. We can then decompose $\mathbb{E}[(S - K)_+]$, which is termed the "stop-loss premium" into a linear combination of stop-loss premiums, such that:

$$\mathbb{E}[(S - K)_+] = \sum_{i=1}^n w_i \mathbb{E}[(X_i - K_i)_+], \quad (4.9)$$

where

$$K_i = F_{X_i}^{-1}(F_s(K)), \text{ for } i = 1, 2, \dots, n. \quad (4.10)$$

$F_s(K)$ is calculated such that the following statement holds true:

$$\sum_{i=1}^n w_i K_i = K. \quad (4.11)$$

A more comprehensive overview of comonotonicity theory can be found in [Dhaene et al. \(2002\)](#) and for proof of the aforementioned theorem refer to [Kaas et al. \(2008\)](#).

Once the intergral in Equation 4.6 is approximated, we can now introduce the notation for the approximate unconditional basket option price as:

$$\bar{C}[K] = \int_0^{+\infty} \bar{C}[K; y] f_H(y) dy, \quad (4.12)$$

where:

the conditional approximation $\bar{C}[K; y]$ is broken down into a sum of weighted convex upper and lower bounds:

$$\bar{C}[K; y] = e^{-rT} \left(z_y \mathbb{E} \left[(S_b^{\text{low}} - K)_+ \right] + (1 + z_y) \mathbb{E} \left[(S_b^{\text{up}} - K)_+ \right] \right). \quad (4.13)$$

Note: $z_y \in [0, 1]$ and $K \geq 0$.

The weights z_y are given as follows:

$$z_y = \frac{\text{Var} [S_b^{\text{up}}] - \text{Var} [S_b]}{\text{Var} [S_b^{\text{up}}] - \text{Var} [S_b^{\text{low}}]}. \quad (4.14)$$

Convex Upper Bound

The conditonal random variable S_b^{up} is expressed by the following, as it follows a multivariate VG process:

$$S_b^{\text{up}} \sim \sum_{i=1}^n w_i S_i(0) e^{(r-q_i+\omega_i)T + \mu_i y + \sigma_i \sqrt{y} \Phi^{-1}(U)}, \quad (4.15)$$

where Φ is the normal cumulative distribution function, U is a uniform random number and the variance of S_b^{up} is expressed as:

$$\text{Var} [S_b^{\text{up}}] = \sum_{i=1}^n \sum_{j=1}^n w_i w_j S_i(0) S_j(0) e^{2rT + (\omega_i - q_i + \omega_j - q_j)T + (\mu_i + \mu_j)y + \frac{\sigma_i^2 + \sigma_j^2}{2} y} (e^{\sigma_i \sigma_j y} - 1). \quad (4.16)$$

The convex upper bound is then given by the following expression:

$$e^{-rT} \mathbb{E} \left[(S_b^{\text{up}} - K)_+ \right] = \sum_{i=1}^n w_i \left(S_i(0) e^{(\omega_i - q_i)T + \left(\mu_i + \frac{\sigma_i^2}{2} \right) y} \Phi(d_{i,1}) - K_i e^{-rT} \Phi(d_{i,2}) \right), \quad (4.17)$$

where

$$d_{i,1} = \frac{\ln \left(\frac{S_i(0)}{K_i} \right) + (r - q_i + \omega_i)T + \mu_i y + \sigma_i^2 y}{\sigma_i \sqrt{y}},$$

and

$$d_{i,2} = d_{i,1} - \sigma_i \sqrt{y}.$$

The strikes K_i are given as:

$$K_i = S_i(0) e^{(r-q_i+\omega_i)T + \mu_i y + \sigma_i \sqrt{y} \Phi^{-1}\left(F_{S_b^{up}}(K)\right)}, \quad (4.18)$$

where the value of $F_{S_b^{up}}(K)$ is determined by ensuring the following relation is true:

$$\sum_{i=1}^n w_i K_i = K, \quad (4.19)$$

where K is the strike price of the option.

The proofs and detailed derivations for Equations 4.16-4.19 can be found in [Linders and Stassen \(2016\)](#).

Convex Lower Bound

The conditional random variable S_b^{low} is expressed by the following, as it also follows a multivariate VG process:

$$S_b^{\text{low}} \sim \sum_{i=1}^n w_i S_i(0) e^{(r-q_i+\omega_i)T + \mu_i y + \frac{\sigma_i^2 y(1-r_i^2)}{2} + r_i \sigma_i \sqrt{y} \Phi^{-1}(U)}, \quad (4.20)$$

where the correlation coefficient r_i is given by

$$r_i = \text{Corr} \left[\Lambda_y, \ln \left(\frac{S_i}{S_i(0)} \mid H = y \right) \right] \quad (4.21)$$

and

$$\Lambda_y \sim \sum_{j=1}^n \lambda_j ((r - q_j + \omega_j)T + \mu_j y + \sigma_j \sqrt{y} B_j), \quad (4.22)$$

where B is a standard Brownian motion.

We can calculate the correlation coefficient r_i by using the following:

$$r_i = \frac{\sum_{j=1}^n \lambda_j \sigma_j \rho_{i,j}}{\sigma_{\Lambda_y}}, \quad (4.23)$$

where r_i is strictly positive and

$$\sigma_{\Lambda_y}^2 = \sum_{i=1}^n \lambda_i^2 \sigma_i^2 + \sum_{i=1, i \neq j}^n \lambda_i \lambda_j \sigma_i \sigma_j \rho_{i,j} \quad \text{for } j = 1, 2, \dots, n. \quad (4.24)$$

Also, we note the weights λ_i of the random variable Λ_y are given by

$$\lambda_j = w_j S_j(0) e^{(r-q_j+\omega_j)T+\mu_j y+\frac{\sigma_j^2 y}{2}} \text{ for } j = 1, 2, \dots, n. \quad (4.25)$$

We note that the variance of S_b^{low} is expressed as:

$$\text{Var} \left[S_b^{\text{low}} \right] = \sum_{i=1}^n \sum_{j=1}^n w_i w_j S_i(0) S_j(0) e^{2rT+(\omega_i-q_i+\omega_j-q_j)T+(\mu_i+\mu_j+\frac{1}{2}(\sigma_i^2+\sigma_j^2))y} (e^{r_i r_j \sigma_i \sigma_j y} - 1). \quad (4.26)$$

The convex lower bound is then given by the following expression:

$$e^{-rT} \mathbb{E} \left[(S_b^{\text{low}} - K)_+ \right] = \sum_{i=1}^n w_i \left(S_i(0) e^{(\omega_i-q_i)T+(\mu_i+\frac{\sigma_i^2}{2})y} \Phi(d_{i,1}) - K_i e^{-rT} \Phi(d_{i,2}) \right), \quad (4.27)$$

where

$$d_{i,1} = \frac{\ln \left(\frac{S_i(0)}{K_i} \right) + (r - q_i + \omega_i)T + \mu_i y + \frac{\sigma_i^2 y(1+r_i^2)}{2}}{r_i \sigma_i \sqrt{y}},$$

and

$$d_{i,2} = d_{i,1} - \sigma_i r_i \sqrt{y}.$$

The strikes K_i are given as:

$$K_i = S_i(0) e^{(r-q_i+\omega_i)T+\mu_i y+\frac{\sigma_i^2 y(1-r_i^2)}{2}+r_i \sigma_i \sqrt{y} \Phi^{-1} \left(F_{S_b^{\text{low}}}(K) \right)}, \quad (4.28)$$

where the value of $F_{S_b^{\text{low}}}(K)$ is determined by ensuring the following relation is true:

$$\sum_{i=1}^n w_i K_i = K, \quad (4.29)$$

where K is the strike price of the option.

The proofs and detailed derivations for Equations 4.21-4.29 can be found in [Linders and Stassen \(2016\)](#).

[Linders and Stassen \(2016\)](#) do not explicitly give the derivation for $\text{Var} [S_b]$ (the variance of the basket). However, the derivation can be found in the Appendix and the final form is given below in Equation 4.30:

$$\text{Var} (S_b) = \sum_{ij} \text{Cov} \left(w_i S_i(0) e^{(r-q_i+\omega_i)T+\mu_i y+\sigma_i \sqrt{y} B_T^i}, w_j S_j(0) e^{(r-q_j+\omega_j)T+\mu_j y+\sigma_j \sqrt{y} B_T^j} \right). \quad (4.30)$$

Chapter 5

Monte Carlo Simulation Study

This chapter presents the numerical testing of the multivariate VG model and the multivariate NIG model in the form of a Monte Carlo simulation study. We make a comparison between the closed-form approximation in Equation 4.12 and the Monte Carlo prices that are calculated using 100 000 simulations. It must be noted that all the coding in this dissertation was performed in the student-licensed version of Matlab R2018a, on a laptop with 1.6 GHz Intel Core i5 processor.

The Monte Carlo study will be carried out for a call option on a basket of three stocks, with expiry being 1 year. The strikes vary between 70 and 110, the risk-free rate is set to 5% and the dividends set to zero, for simplicity. All stocks have initial prices of 100 and they have a weighting of 0.2, 0.6 and 0.2 respectively. The dynamic parameters for each stock vary according to the model being implemented and thus are stated in the relevant section (5.1 for VG and 5.2 for NIG).

The results presented in Tables 5.1-5.5 show the prices calculated using the approximation detailed in Equation 4.12 and the Monte Carlo prices for the multivariate VG model, and Tables 5.6-5.10 show the same results, but for the multivariate NIG model. The percentage relative error between the two prices (analytical approximation and Monte Carlo) is also calculated and is done so for 5 different strike prices, as a way of assessing the model to a fuller extent.

5.1 Multivariate Variance Gamma

The dynamic parameters of the multivariate VG model are given as: volatilities $\sigma = \{\sigma_1, \sigma_2, \sigma_3\} = \{0.1, 0.1, 0.2\}$ and the drift parameters $\mu = \{\mu_1, \mu_2, \mu_3\} = \{0.2, -0.1, 0.1\}$. The value for the parameter ν is alternated between 0.2 and 0.5 and the value of the correlation coefficient ρ is alternated between 0 and 0.5.

In Tables 5.1-5.5, we notice a few different trends as the parameter values are varied. Firstly, a prevalent trend amongst higher strikes is observed: a higher correlation coefficient results in higher option prices, for the same strike. This trend is

observed for most cases, with the exception of the low strikes of 70 and 80, as can be seen in Tables 5.1 and 5.4. The result of a higher correlation coefficient influences the volatility of the basket as whole, by increasing it. This is the driving force behind increased options prices and it is what we would expect. This trend is evident in all of the tables given below.

Looking at Tables 5.1 and 5.2, we notice that the prices in Table 5.2 are slightly higher than in Table 5.1. These tables have the same subordinator variance (ν), but the weighting of the stocks is changed, which suggest that when the stock with the higher volatility is weighted more heavily than the other, it results in higher option prices. The same trend is observed in Tables 5.3 and 5.4, where again the weights are varied, but the subordinator variance is kept constant at 0.5.

Tables 5.1 and 5.3 both weight the stocks the same way, but the parameter ν is 0.2 in Table 5.1 and 0.5 in Table 5.3. The observed trend here is that the larger ν has resulted in higher options prices but also that the relative errors are less than those found in Table 5.1. We note that the same can be said for Tables 5.2 and 5.4.

If we analyse Table 5.5, we see that ν is 0.5 and the weights of the stocks are 0.2, 0.2 and 0.6, respectively. The difference between this table and Table 5.4 is that the volatilities are now all equal to 0.1 (as opposed to 0.1, 0.1 and 0.2). We see that the prices in Table 5.5 are lower than those in Table 5.4. This, once again, illustrates the observation that was made earlier indicating that assigning heavier weighting to the stock with the higher volatility leads to higher options prices.

Looking at the entire set of results, the relative errors between the analytical approximation and the Monte Carlo prices never exceed 1.56%, with the vast majority of results lying below the 1% relative error bound. This suggests that the analytical approximation implemented with the multivariate VG model, provides an expression for a basket call option that is accurate, in terms of this Monte Carlo simulation test.

Tab. 5.1: A comparison of the simulation results and analytical approximations for the VG model with parameters $\nu = 0.2$, weights $w = \{0.2, 0.6, 0.2\}$ and $\sigma = \{0.1, 0.1, 0.2\}$, for maturity of 1 year

Correlation Coefficient (ρ)	Strike	Analytical Approximation	Monte Carlo Price	Relative Error (%)
0	70	33.41	33.45	0.11888
	80	23.90	23.94	0.16499
	90	14.45	14.49	0.26862
	100	5.93	5.97	0.63023
	110	1.28	1.30	1.55607
0.5	70	33.41	33.40	0.04064
	80	23.92	23.91	0.05142
	90	14.64	14.63	0.09475
	100	6.73	6.72	0.22780
	110	2.14	2.14	0.13351

Tab. 5.2: A comparison of the simulation results and analytical approximations for the VG model with parameters $\nu = 0.2$, weights $w = \{0.2, 0.2, 0.6\}$ and $\sigma = \{0.1, 0.1, 0.2\}$, for maturity of 1 year

Correlation Coefficient (ρ)	Strike	Analytical Approximation	Monte Carlo Price	Relative Error (%)
0	70	33.41	33.37	0.12411
	80	23.93	23.89	0.16796
	90	14.84	14.81	0.20435
	100	7.62	7.61	0.18159
	110	3.42	3.41	0.16108
0.5	70	33.42	33.48	0.17255
	80	24.01	24.07	0.25492
	90	15.22	15.28	0.39357
	100	8.32	8.38	0.64525
	110	4.09	4.12	0.87581

Tab. 5.3: A comparison of the simulation results and analytical approximations for the VG model with parameters $\nu = 0.5$, weights $w = \{0.2, 0.6, 0.2\}$ and $\sigma = \{0.1, 0.1, 0.2\}$, for a maturity of 1 year

Correlation Coefficient (ρ)	Strike	Analytical Approximation	Monte Carlo Price	Relative Error (%)
0	70	33.38	33.42	0.12833
	80	23.88	23.91	0.13870
	90	14.44	14.47	0.16799
	100	5.88	5.89	0.26296
	110	1.30	1.31	0.93325
0.5	70	33.38	33.42	0.11869
	80	23.90	23.94	0.12939
	90	14.65	14.67	0.13717
	100	6.64	6.64	0.00162
	110	2.12	2.11	0.05793

Tab. 5.4: A comparison of the simulation results and analytical approximations for the VG model with parameters $\nu = 0.5$, weights $w = \{0.2, 0.2, 0.6\}$ and $\sigma = \{0.1, 0.1, 0.2\}$, for a maturity of 1 year

Correlation Coefficient (ρ)	Strike	Analytical Approximation	Monte Carlo Price	Relative Error
0	70	33.39	33.41	0.07225
	80	23.91	23.93	0.07339
	90	14.80	14.81	0.08013
	100	7.74	7.73	0.02555
	110	3.89	3.88	0.28175
0.5	70	33.40	33.33	0.20274
	80	23.99	23.91	0.31401
	90	15.16	15.08	0.51685
	100	8.39	8.33	0.75062
	110	4.49	4.45	1.08143

Tab. 5.5: A comparison of the simulation results and analytical approximations for the VG model with parameters $\nu = 0.5$, weights $w = \{0.2, 0.2, 0.6\}$ and $\sigma = \{0.1, 0.1, 0.1\}$, for a maturity of 1 year

Correlation Coefficient (ρ)	Strike	Analytical Approximation	Monte Carlo Price	Relative Error (%)
0	70	33.39	33.43	0.13362
	80	23.89	23.92	0.14694
	90	14.40	14.42	0.17647
	100	6.04	6.05	0.22662
	110	2.11	2.12	0.53364
0.5	70	33.39	33.44	0.14234
	80	23.89	23.93	0.15943
	90	14.47	14.50	0.20290
	100	6.53	6.54	0.22849
	110	2.58	2.59	0.33102

5.2 Multivariate Normal Inverse Gaussian

The dynamic parameters of the multivariate NIG model are given as: volatilities $\sigma = \{\sigma_1, \sigma_2, \sigma_3\} = \{0.1, 0.1, 0.2\}$ and the drift parameters $\mu = \{\mu_1, \mu_2, \mu_3\} = \{-0.02, -0.01, -0.03\}$. The value for the parameter ν is alternated between 0.2 and 0.5 and the value of the correlation coefficient ρ is alternated between 0 and 0.5.

We note that when using the higher correlation coefficients, higher options prices for the same strike are achieved for most cases, in Tables 5.6-5.10. This trend was also observed for the case of the multivariate VG. However, as was seen in some cases of the multivariate VG case, there are a few exceptions in the case of lower strikes. This is observed in Tables 5.7- 5.9, all for strikes of 70. Increasing the correlation coefficient increases the volatility of the basket as a whole, which is the cause of higher options prices, which we observe to be the general trend.

If we examine Tables 5.6 and 5.7, we note that both tables have the same variance of subordinator ($\nu = 0.2$), but a different weighting for the three stocks. Table 5.7 weights the stock with the highest volatility more heavily ($\sigma_3 = 0.2, w_3 = 0.6$) and we observe that this table has higher options prices than in Table 5.6. The same trend is evident in Tables 5.8 and 5.9, where the variance of subordinator (ν) is now 0.5, and Table 5.9 weights the stock with the highest volatility more heavily. Once again, this trend was observed earlier for the VG case.

Examining Tables 5.6 and 5.8, we note the weights of the stocks is the same for

both tables, the volatilities are also kept the same, but the variance of the subordinator is changed. It is 0.2 for Table 5.6 and 0.5 for Table 5.8. We notice here that the trend differs from that found in the multivariate VG case, whereby the options prices are actually found to decrease with increasing subordinator variance. This is also found when comparing Tables 5.7 and 5.9. This trend agrees with the results found by Wu et al. (2009) for the pricing of an arithmetic basket option. Table 5.8 exhibits lower relative errors than those found in Table 5.6. This agrees with the observation made in the multivariate VG case in section 5.1.

If we now analyse the results found in Tables 5.9 and 5.10, we note that the subordinator variance is kept constant at 0.5, the weighting is the same, but now the volatility of each of the respective stocks has been altered. In Table 5.9, we note the volatilities are $\sigma = \{0.1, 0.1, 0.2\}$, but in Table 5.10, the volatilities are all made equal. Table 5.9 shows higher options prices, which aligns with the observation made when comparing Table 5.6 with Table 5.7 and Table 5.8 with Table 5.9 - when the stock with higher volatility is weighted more heavily, it results in higher options prices.

Tables 5.6-5.10 exhibit that the majority of the relative errors between the analytical approximation and the Monte Carlo prices never exceed 1%. This is with the exception of two results, which still lie below a relative error of 1.5%. This suggests that the analytical approximation, when implemented with the multivariate NIG model, provides an accurate expression for the price of a basket call option, in terms of this Monte Carlo test.

In comparison to the multivariate VG, the highest relative error of the NIG results is 1.497%, and for VG is 1.556%. These maximum errors are close, but suggest for this experiment, that the NIG results were slightly more accurate. This is, of course, a result of the chosen parameters and could vary for a different choice of parameters. However, the general note we make is that the relative errors from both sets of results (VG and NIG) are very close, with no significant difference.

Tab. 5.6: A comparison of the simulation results and analytical approximations for the NIG model with parameters $\nu = 0.2$, weights $w = \{0.2, 0.6, 0.2\}$ and $\sigma = \{0.1, 0.1, 0.2\}$, for maturity of 1 year

Correlation Coefficient (ρ)	Strike	Analytical Approximation	Monte Carlo Price	Relative Error (%)
0	70	36.27	36.25	0.05438
	80	26.76	26.74	0.07400
	90	17.28	17.26	0.11049
	100	8.31	8.31	0.07939
	110	2.22	2.23	1.46952
0.5	70	36.27	36.26	0.03876
	80	26.77	26.76	0.05137
	90	17.40	17.39	0.09305
	100	8.94	8.92	0.30781
	110	3.22	3.19	0.79641

Tab. 5.7: A comparison of the simulation results and analytical approximations for the NIG model with parameters $\nu = 0.2$, weights $w = \{0.2, 0.2, 0.6\}$ and $\sigma = \{0.1, 0.1, 0.2\}$, for maturity of 1 year

Correlation Coefficient (ρ)	Strike	Analytical Approximation	Monte Carlo Price	Relative Error (%)
0	70	36.94	36.96	0.05312
	80	27.46	27.48	0.07194
	90	18.21	18.24	0.11443
	100	10.09	10.11	0.18813
	110	4.48	4.50	0.40681
0.5	70	36.95	36.91	0.10149
	80	27.53	27.49	0.14168
	90	18.50	18.46	0.23660
	100	10.73	10.68	0.44438
	110	5.26	5.22	0.66079

Tab. 5.8: A comparison of the simulation results and analytical approximations for the NIG model with parameters $\nu = 0.5$, weights $w = \{0.2, 0.6, 0.2\}$ and $\sigma = \{0.1, 0.1, 0.2\}$, for a maturity of 1 year

Correlation Coefficient (ρ)	Strike	Analytical Approximation	Monte Carlo Price	Relative Error (%)
0	70	34.18	34.18	0.00810
	80	24.68	24.68	0.00255
	90	15.25	15.25	0.01639
	100	6.57	6.57	0.04577
	110	1.40	1.40	0.28700
0.5	70	34.18	34.20	0.05762
	80	24.71	24.72	0.06301
	90	15.45	15.45	0.04113
	100	7.28	7.28	0.08698
	110	2.27	2.27	0.15396

Tab. 5.9: A comparison of the simulation results and analytical approximations for the NIG model with parameters $\nu = 0.5$, weights $w = \{0.2, 0.2, 0.6\}$ and $\sigma = \{0.1, 0.1, 0.2\}$, for a maturity of 1 year

Correlation Coefficient (ρ)	Strike	Analytical Approximation	Monte Carlo Price	Relative Error
0	70	34.38	34.43	0.15357
	80	24.94	24.99	0.20571
	90	15.86	15.90	0.29256
	100	8.11	8.13	0.27514
	110	3.23	3.23	0.10156
0.5	70	34.41	34.43	0.06180
	80	25.05	25.07	0.06794
	90	16.20	16.21	0.05369
	100	8.77	8.77	0.01851
	110	3.93	3.92	0.15908

Tab. 5.10: A comparison of the simulation results and analytical approximations for the NIG model with parameters $\nu = 0.5$, weights $w = \{0.2, 0.2, 0.6\}$ and $\sigma = \{0.1, 0.1, 0.1\}$, for a maturity of 1 year

Correlation Coefficient (ρ)	Strike	Analytical Approximation	Monte Carlo Price	Relative Error (%)
0	70	34.18	34.15	0.08785
	80	24.67	24.64	0.12175
	90	15.22	15.19	0.19749
	100	7.27	7.24	0.40986
	110	1.42	1.40	1.49706
0.5	70	34.18	34.19	0.02925
	80	24.69	24.69	0.01537
	90	15.32	15.31	0.06532
	100	7.72	7.71	0.14563
	110	2.08	2.06	0.83686

Chapter 6

Calibration

This chapter details the procedure followed in order to determine the risk-neutral parameters for each of the financial models described in Chapter 2. The purpose of calibration is to match the model prices to observed market prices, as accurately as possible. This is done by backing out the optimal risk-neutral parameters of the model, so that the error between observed market and model prices is minimised, in relation to some error measure (Cont and Tankov, 2003). In order to perform the calibration, we require quoted market prices. Pricing data for basket options, and also other multi-asset options, is often not observable in the market and thus quoted vanilla options data is used as the observed market prices instead. Once the model parameters have been determined, exotic options can be priced.

6.1 Calibration Method: Non-Linear Least Squares

To restate the calibration problem in a more mathematical sense, let us denote the set of model prices for n vanilla call options: $\{C_0^{\text{model}}(T_i, K_i; \theta) \text{ for } i = 1, \dots, n\}$. Here, θ is a vector of model parameters. Let us also observe a set of quoted market prices for n liquid vanilla call options: $\{C_0^{\text{market}}(T_i, K_i) \text{ for } i = 1, \dots, n\}$. Both sets consist of vanilla call options valued at $t = 0$, with various expiries T_1, T_2, \dots, T_n and strikes K_1, K_2, \dots, K_n .

Ideally, the theory behind calibration is to find θ such that we achieve Equation 6.1. Typically, however, we have more options than parameters, so we cannot solve Equation 6.1 exactly. Hence, we use a least squares criterion to solve for one set of 'optimal' parameters (i.e. θ).

$$C_0^{\text{model}}(T_i, K_i; \theta) = C_0^{\text{market}}(T_i, K_i) \text{ for } i \in I. \quad (6.1)$$

The models used in this dissertation are exponential Lévy models, i.e. $S_t = e^{X_t}$, where X_t is the Lévy model characterised by the Lévy triplet (σ, ν, μ) .

This process of non-linear least squares calibration involves the minimisation of the quadratic pricing error between the observed market and the model prices, given in a general case by [Cont and Tankov \(2003\)](#) as:

$$\text{LSE} = \arg \min_{\theta} \sum_{i=1}^N w_i |C_i^{\theta}(T_i, K_i; \theta) - C_i|^2, \quad (6.2)$$

where the C^{θ} is the set of vanilla call options priced using the exponential Lévy model with triplet (σ, μ, ν) , corresponding to the set of martingale measures and w_i is a weighting factor.

We use the root mean square error (RMSE) as the specific case of a nonlinear least squares method. The RMSE is given by [Luciano and Schoutens \(2006\)](#) as:

$$\text{RMSE} = \sqrt{\sum_i \frac{(\text{Market Price} - \text{Model Price})^2}{n}}, \quad (6.3)$$

where n is the number of derivatives.

This method has been widely used in the field of mathematical finance, including the use by [Schoutens \(2003\)](#), [Carr et al. \(2003\)](#), [Kyprianou et al. \(2006\)](#), [Luciano and Schoutens \(2006\)](#), [Ballotta and Bonfiglioli \(2016\)](#) and [Linders and Stassen \(2016\)](#).

For our purposes, we intend to price a basket option where the underlyings are the stocks that constitute the KBW Bank Index, as previously mentioned, and thus we use three quoted vanilla call options on each of the stocks underlying the index that were obtained from Bloomberg (i.e. a total of 72 vanilla call options, all dated 16 January 2019). This means that we are calibrating with the intention of simultaneously backing out 49 parameters: $\mu_1, \mu_2, \dots, \mu_n, \sigma_1, \sigma_2, \dots, \sigma_n$ and ν , where $n = 24$ (the KBW Bank Index consists of 24 banking stocks). We calibrate two exponential Lévy models: the multivariate VG model and the multivariate NIG model.

6.1.1 Variance Gamma (VG) Model

The calibrated parameters for the VG model are shown in [Table 6.1](#), as well as the minimised RMSE for each stock. The RMSE for each of the stocks is very small, with the largest RMSE being 0.159 and the smallest RMSE being a mere 0.002. This suggests that the model-priced vanilla call options fit the observed vanilla call options curves very well, as is also illustrated in [Figure 6.1](#).

Tab. 6.1: Calibrated parameters of the Lévy triplet for the VG model and the resulting minimised RMSE

Stock	$S_i(0)$	μ_i	σ_i	RMSE
Bank of America	26.55	-0.21664	0.24743	0.015
BB&T	46.34	-0.36864	0.17205	0.045
Bank of New York Mellon	49.41	-0.22933	0.23786	0.025
Citigroup Inc	61.38	-0.21504	0.23927	0.030
Citizens Financial Group	33.10	-0.27957	0.27266	0.020
Comerica	74.04	-0.30090	0.27763	0.019
Capital One Financial	81.52	-0.20052	0.25769	0.032
Fifth Third Bancorp	25.46	-0.25330	0.25124	0.009
First Republic Bank	94.33	-0.25127	0.27254	0.042
Huntington Bancshares	12.88	-0.18315	0.26007	0.024
JPMorgan Chase & Co	101.68	-0.27958	0.19080	0.047
KeyCorp	16.31	-0.17249	0.30104	0.010
M&T Bank	151.45	-0.25340	0.23394	0.049
Northern Trust	86.95	-0.19842	0.27031	0.028
New York Community Bancorp	10.13	-0.27518	0.26841	0.010
People's United Financial Inc	15.54	0.22081	0.17714	0.060
PNC Financial Services Group	121.12	-0.23823	0.24121	0.044
Regions Financial	15.11	-0.10629	0.31801	0.002
SVB Financial Group	218.71	-0.27836	0.41390	0.109
SunTrust Banks	55.99	-0.29431	0.22678	0.026
State Street	68.66	-0.26460	0.30926	0.027
US Bancorp	47.97	-0.25989	0.18852	0.030
Wells Fargo & Co	47.67	-0.21087	0.23029	0.020
Zions Bancorp	44.81	0.13292	0.26157	0.159
Variance of subordinator (ν)	0.216538			

Note that $S_i(0)$ is the observed initial stock price on 16 January 2019, μ_i the drift of the Brownian motion and σ_i the volatility of the Brownian motion (as per the Lévy triplet (σ, ν, μ)).

6.1.2 Normal Inverse Gaussian (NIG) Model

The calibrated parameters for the NIG model are shown in Table 6.2 as well as the minimised RMSE for each stock. The RMSE for each of the stocks is also very small,

with the largest RMSE being 0.291 and the smallest RMSE being 0.008. This suggests that the model-priced vanilla call options fit the observed vanilla call options curves very well, but in comparison to the VG model, not quite as accurately, see Figures 6.1 and 6.2.

Tab. 6.2: Calibrated parameters of the Lévy triplet for the NIG model and the resulting minimised RMSE

Stock	$S_i(0)$	μ_i	σ_i	RMSE
Bank of America	26.55	-0.02697	0.20646	0.020
BB&T	46.34	-0.0231	0.18688	0.095
Bank of New York Mellon	49.41	-0.02623	0.2124	0.053
Citigroup Inc	61.38	-0.02557	0.20321	0.034
Citizens Financial Group	33.10	-0.03295	0.23845	0.014
Comerica	74.04	-0.03186	0.21972	0.117
Capital One Financial	81.52	-0.02743	0.20932	0.065
Fifth Third Bancorp	25.46	-0.02865	0.20993	0.009
First Republic Bank	94.33	-0.03113	0.21435	0.033
Huntington Bancshares	12.88	-0.02924	0.22603	0.019
JPMorgan Chase & Co	101.68	-0.02107	0.18636	0.105
KeyCorp	16.31	-0.03552	0.24966	0.017
M&T Bank	151.45	-0.02552	0.20807	0.027
Northern Trust	86.95	-0.03168	0.24058	0.058
New York Community Bancorp	10.13	-0.03252	0.23576	0.008
People's United Financial Inc	15.54	-0.02701	0.24619	0.053
PNC Financial Services Group	121.12	-0.02635	0.20204	0.068
Regions Financial	15.11	-0.03762	0.25986	0.025
SVB Financial Group	218.71	-0.06232	0.32811	0.382
SunTrust Banks	55.99	-0.02697	0.21591	0.054
State Street	68.66	-0.03673	0.23254	0.112
US Bancorp	47.97	-0.02077	0.1863	0.087
Wells Fargo & Co	47.67	-0.02459	0.20345	0.048
Zions Bancorp	44.81	-0.02838	0.23876	0.291
Variance of subordinator (ν)				
0.081130				

Note that $S_i(0)$ is the observed initial stock price on 16 January 2019, μ_i the drift of the Brownian motion and σ_i the volatility of the Brownian motion (as per the Lévy triplet (σ, ν, μ)).

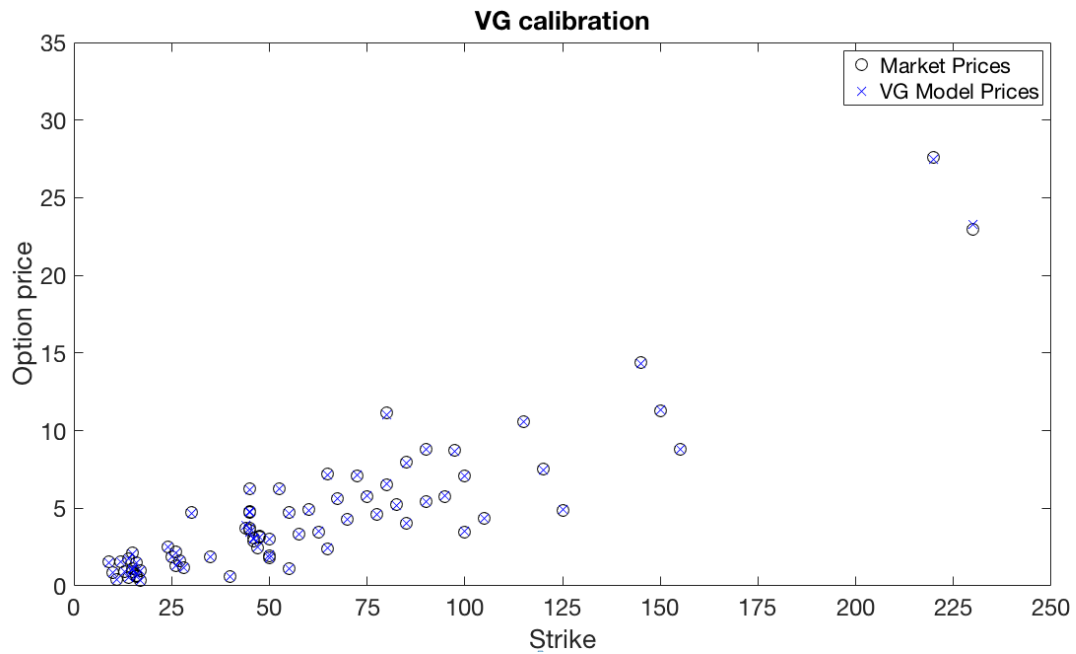


Fig. 6.1: Calibration of the VG model prices (crosses) to vanilla call options prices (circles) on 16 January 2019

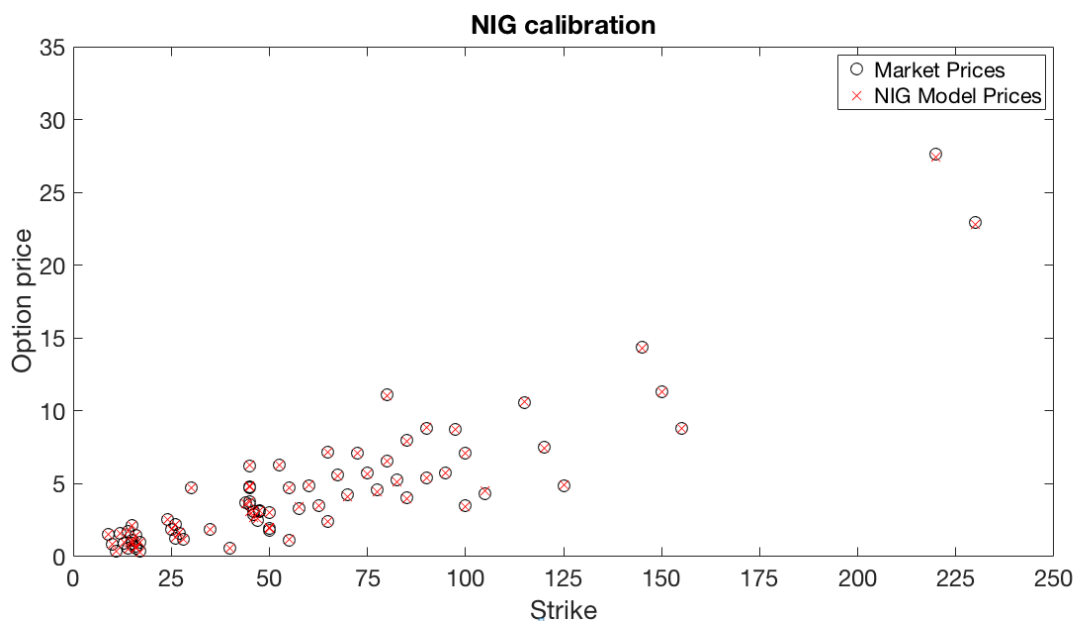


Fig. 6.2: Calibration of the NIG model prices (crosses) to vanilla call options prices (circles) on 16 January 2019

We discern that there have been calibration constraints imposed during this procedure, i.e. the model is preassigned as an exponential Lévy model and also there are only a finite number of observed options prices available. This suggests that finding an exact solution for the calibrated parameters may not be possible (Cont and Tankov, 2003). Therefore, the calibration represents the best-possible approximation of market prices, which explains why the RMSE observed in Tables 6.1 and 6.2 are not zero. The precision of this method may also be influenced by starting points used in the optimization process. This is explored in Cont and Tankov (2003), although the difference in precision between different starting points is not significantly large.

Chapter 7

Pricing of a Basket Option

In this chapter, we use two pricing methods to price a basket option consisting of the 24 banking stocks that make up the KBW Bank Index. The first method is the standard Monte Carlo method and the second method is an analytical approximation method that was derived by [Linders and Stassen \(2016\)](#). The Monte Carlo method is implemented using both VG and NIG models in order to compare the two exponential Lévy models in terms of fit to market data. The VG model is then compared to the Monte Carlo method in terms of accuracy and efficiency.

The basket option that is priced in this chapter is the weighted sum of the banking stocks that make up the KBW Bank Index. The specific weighting used is the same as that used to weight the index, and is called modified market-capitalisation. The calculation of the weightings of each stock is described online on the Nasdaq website ([Nasdaq, 2018](#)). In brief, the stocks are weighted by market capitalisation and adjusted for share price. We do this in order to compare the model basket option prices to quoted market prices of options on the index.

7.1 Comparison of Models using the Monte Carlo Method

In Chapter 5, both the multivariate VG and multivariate NIG models were calibrated to real market data and the parameters that make up the Lévy triplet in each case were determined. We now use these calibrated parameters to price a basket option on 24 underlying banking stocks using both the VG and NIG models. Note that the models were calibrated to vanilla options data, as seen in Chapter 6.

Both models were implemented along with the Monte Carlo pricing method for various maturities ($T = 156, 163$ and 349 days, as this was the data that was available) and a range of strikes, for 1 000 000 simulations. The Monte Carlo prices and the market prices are compared in Table 7.2 for the multivariate VG model and in Table 7.3 for the multivariate NIG model. We note that the 156 and 163 day maturities are only a week apart and therefore we expect to observe similar market

prices for these two maturities, which is evident in Tables 7.2 and 7.3. The absolute errors between the Monte Carlo prices and observed market prices are detailed for each strike and maturity in these tables, as well as the overall RMSE. By drawing a comparison between the multivariate NIG prices versus the multivariate VG prices, in relation to the market prices, we observe that the multivariate VG model fits the market prices better for the 349 day maturity, the multivariate NIG model fits the market prices better for the 156 and 163 day maturity, as is summarised by the RMSE stated in Table 7.1. Also, both models seem to follow one another, but do not fit the market prices exactly. This is illustrated by how closely the model prices fit the quoted market price curves. The reason behind this could be the fact that both the models fail to capture the interdependence between asset prices correctly.

However, looking at Figures 7.1, 7.2 and 7.3, where the multivariate VG and multivariate NIG model Monte Carlo prices in reference to the observed market prices are compared, we make the following observations: it seems that the models fit market prices more accurately for shorter maturities, as is evident by the decreasing RMSE for shorter maturities. For the 156 day maturity, the RMSE for the multivariate VG model is 0.640 and for the multivariate NIG model is 0.617; whereas the RMSEs for the 349 day maturity are larger than 1, at 1.939 for the multivariate VG model and 2.866 for the multivariate NIG model.

Tab. 7.1: A Summary of the RMSE for basket options with various maturities and priced using the multivariate VG and multivariate NIG models

Model	RMSE		
	156 day	163 day	349 day
Variance Gamma (VG)	0.640	0.757	1.939
Normal Inverse Gaussian (NIG)	0.617	0.604	2.866

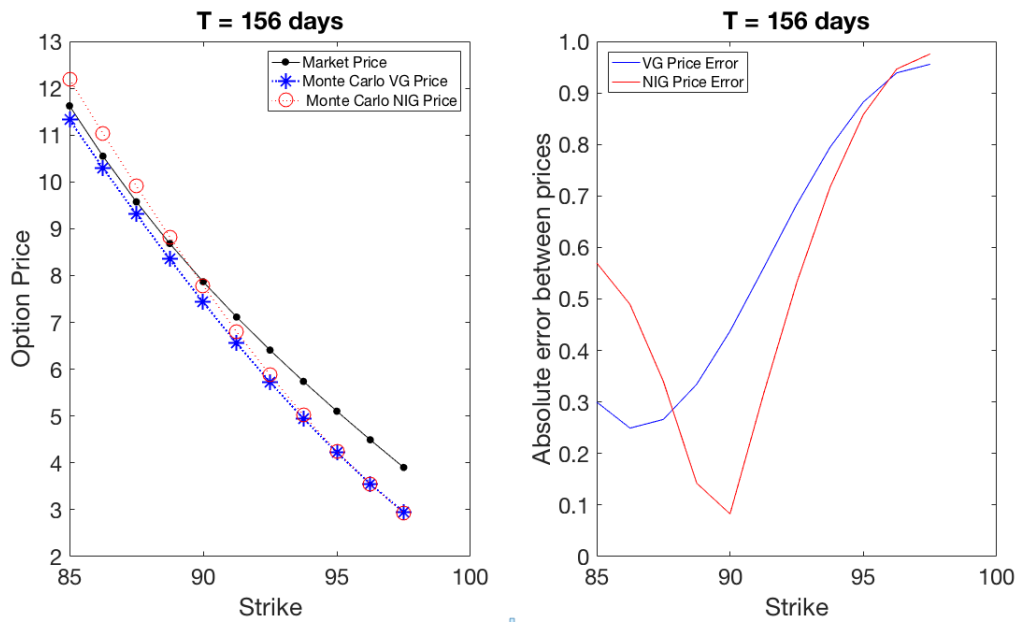


Fig. 7.1: Monte Carlo prices of basket options for both multivariate VG (asterisks) and multivariate NIG models (circles) vs market prices (dots) on 16 January 2019, with a time to maturity of 156 days

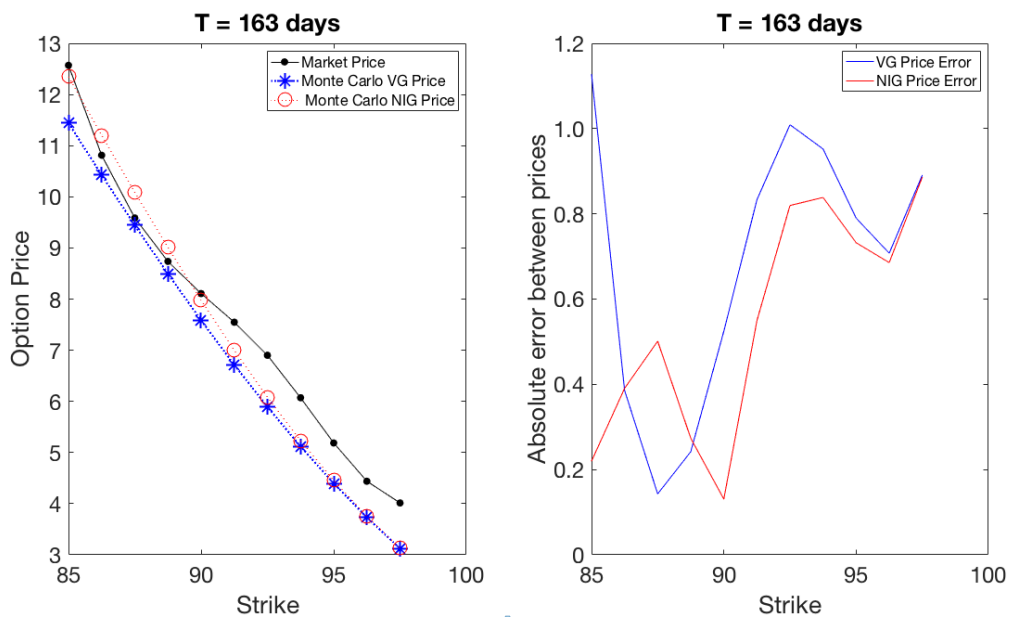


Fig. 7.2: Monte Carlo prices of basket options for both multivariate VG (asterisks) and multivariate NIG models (circles) vs market prices (dots) on 16 January 2019, with a time to maturity of 163 days

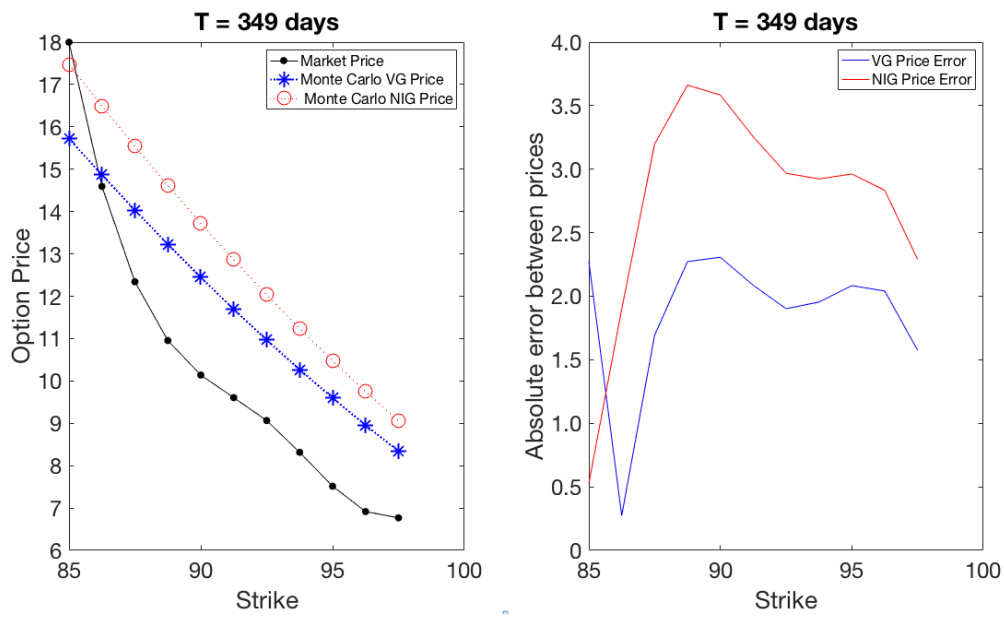


Fig. 7.3: Monte Carlo prices of basket options for both multivariate VG (asterisks) and multivariate NIG models (circles) vs market prices (dots) on 16 January 2019, with a time to maturity of 349 days

The results illustrated in Figures 7.1-7.3, are detailed in Tables 7.2 and 7.3 below.

Tab. 7.2: Monte Carlo price using the multivariate VG model vs the market price for basket options priced on 16 January 2019 for various maturities

Time to Maturity (days)	Strike	Monte Carlo Price	Market Price	Absolute Error	RMSE
156	85.00	11.32	11.62	0.300	0.640
	86.25	10.30	10.55	0.249	
	87.50	9.31	9.57	0.266	
	88.75	8.35	8.68	0.335	
	90.00	7.43	7.87	0.438	
	91.25	6.55	7.11	0.559	
	92.50	5.72	6.41	0.683	
	93.75	4.95	5.74	0.795	
	95.00	4.22	5.10	0.882	
	96.25	3.55	4.49	0.939	
	97.50	2.95	3.90	0.956	
163	85.00	11.44	12.57	1.13	0.757
	86.25	10.43	10.81	0.386	
	87.50	9.44	9.59	0.143	
	88.75	8.49	8.74	0.242	
	90.00	7.58	8.11	0.525	
	91.25	6.72	7.55	0.833	
	92.50	5.89	6.90	1.009	
	93.75	5.12	6.07	0.952	
	95.00	4.40	5.19	0.780	
	96.25	3.73	4.44	0.708	
	97.50	3.12	4.01	0.891	
349	85.00	15.72	18.00	2.274	1.939
	86.25	14.87	14.59	0.273	
	87.50	14.03	12.34	1.692	
	88.75	13.23	10.95	2.273	
	90.00	12.45	10.14	2.307	
	91.25	11.69	9.61	2.086	
	92.50	10.97	9.07	1.902	
	93.75	10.27	8.31	1.954	
	95.00	9.60	7.51	2.084	
	96.25	8.96	6.92	2.041	
	97.50	8.34	6.77	1.575	

Tab. 7.3: Monte Carlo price using the multivariate NIG model vs the market price for basket options priced on 16 January 2019 for various maturities

Time to Maturity (days)	Strike	Monte Carlo Price	Market Price	Absolute Error	RMSE
156	85.00	12.19	11.62	0.570	0.617
	86.25	11.04	10.55	0.489	
	87.50	9.91	9.57	0.340	
	88.75	8.83	8.68	0.142	
	90.00	7.79	7.87	0.083	
	91.25	6.80	7.11	0.314	
	92.50	5.88	6.41	0.532	
	93.75	5.02	5.74	0.717	
	95.00	4.25	5.10	0.858	
	96.25	3.55	4.49	0.946	
	97.50	2.93	3.90	0.976	
163	85.00	12.35	12.57	0.220	0.604
	86.25	11.20	10.81	0.391	
	87.50	10.09	9.59	0.501	
	88.75	9.01	8.74	0.274	
	90.00	7.98	8.11	0.131	
	91.25	7.00	7.55	0.549	
	92.50	6.08	6.90	0.820	
	93.75	5.23	6.07	0.838	
	95.00	4.45	5.19	0.732	
	96.25	3.75	4.44	0.686	
	97.50	3.13	4.01	0.886	
349	85.00	17.47	18.00	0.527	2.866
	86.25	16.49	14.59	1.898	
	87.50	15.53	12.34	3.197	
	88.75	14.62	10.95	3.662	
	90.00	13.72	10.14	3.584	
	91.25	12.86	9.61	3.255	
	92.50	12.03	9.07	2.968	
	93.75	11.23	8.31	2.924	
	95.00	10.47	7.51	2.962	
	96.25	9.75	6.92	2.835	
	97.50	9.06	6.77	2.290	

7.2 Comparison of Pricing Methods

In Chapter 4, the closed-form approximation for the price of a basket option that was derived by [Linders and Stassen \(2016\)](#) was presented. Then, in Chapter 6, the models were calibrated to observed market data that was obtained from Bloomberg to determine the risk-neutral parameters. The closed-form approximation by [Linders and Stassen \(2016\)](#) is implemented and termed the "analytical approximation". This is compared to the Monte Carlo pricing method in terms of efficiency and accuracy. The Monte Carlo prices are calculated by running 100 000 simulations. In this chapter, both the multivariate VG model and the multivariate NIG model are implemented.

The analytical approximation for a KBW Bank Index call option on 16 January 2019 was applied for a maturity of 156, 163 and 349 days - as mentioned in the previous chapter, this was the only available data. In Figures 7.4 - 7.15, the red crosses represent the analytical approximation prices and the black dots are market prices. The blue circles represent the Monte Carlo prices, with three standard deviation error bounds around these prices denoted by dashed green lines.

7.2.1 Multivariate Variance Gamma Model

The multivariate VG model was used in the analytical approximation and Monte Carlo prices shown in Figures 7.4 - 7.9. Figures 7.5, 7.7 and 7.9 are the zoomed-in versions of Figures 7.4, 7.6 and 7.8, respectively. The grey dotted-lined circle in Figures 7.4, 7.6 and 7.8 show the area that is zoomed-in and displayed in Figures 7.5, 7.7 and 7.9. This is done to illustrate the Monte Carlo error bounds more clearly, as the standard deviation of the Monte Carlo prices is very small and difficult to see in all of the figures.

Breaking down each maturity, we analyse the results for the 156 and 163 day maturity displayed in Figures 7.4-7.7 and notice that the fit of the analytical approximation to the Monte Carlo is very similar (as we expect since they are only a week apart), with the RMSE of the 156 day being 0.493 and the 163 day being 0.463. The option prices for both these maturities fall outside of the three standard deviation error bounds, suggesting that the option prices of the analytical approximation are not accurate in terms of the Monte Carlo prices. We also note that by looking at the error graphs in Figure 7.4 and 7.6, the absolute error between the analytical approximation and the Monte Carlo prices decreases as the strike increases. Note, at-the-money strike is 94.89.

For the longest maturity, 349 days, the analytical approximation produces the best results in terms of converging toward Monte Carlo. As is made clearer in Fig-

ure 7.9, the analytical approximation prices fit within the standard deviation error bounds and sit very closely to the Monte Carlo circles. Table 7.5 details the absolute errors and it is shown that the highest absolute error is only 0.031, which means that the analytical approximation performs better for longer-dated maturities, in terms of fit to the Monte Carlo prices. Notice, also, that the absolute errors also tend to decrease as the strikes increase, the same trend that was found for the results of the 156 and 163 day maturities - see Figure 7.8.

Tab. 7.4: A Summary of the RMSE and absolute errors between the Monte Carlo and analytical approximation prices for basket options with various maturities, when implemented for the multivariate VG model

Error	Days to Maturity		
	156 day	163 day	349 day
RMSE	0.493	0.463	0.026
Highest absolute error	0.549	0.516	0.031
Lowest absolute error	0.391	0.370	0.019

The general trend that can be observed is that as the days to maturity increase, the convergence of the analytical approximation prices to the Monte Carlo prices improves. Note that Monte Carlo prices are viewed as the "true" prices more so than the market prices because the model underpinning the market prices is unknown and therefore its accuracy cannot be assessed.

Evidently, the analytical approximation falls out of these error bounds for options that have shorter expiries (i.e. 156 and 163 days), whereas, the 349 day maturity option prices fit well within the error bounds. In Figures 7.4, 7.6 and 7.8, we also notice that the absolute errors between the Monte Carlo prices and the analytical approximations are decreasing as the strike increases. If we analyse the numbers presented in Table 7.4, we see that the root mean square error (RMSE), which is based on 11 options, is smallest for the 349 day expiry (RMSE = 0.026) and largest for the shortest expiry (156 day RMSE = 0.493). The trend is also illustrated in Table 7.4 by the highest and lowest relative errors between the analytical approximation and the Monte Carlo price, for different maturities. For more detailed prices, see Table 7.5. All of this evidence suggests that the analytical approximation performs better for longer-dated maturities, in pricing basket options.

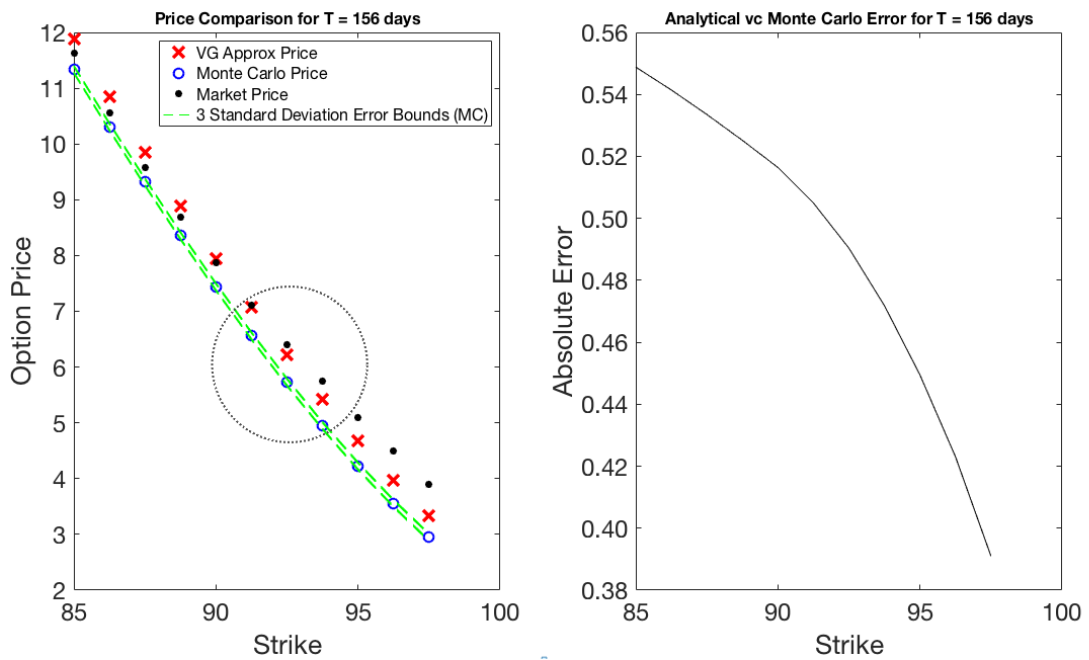


Fig. 7.4: A price comparison of Monte Carlo prices (circles), analytical approximation prices (crosses) and market prices (dots), for a call option on the KBW Bank Index on 16 January 2019 with maturity of 156 days

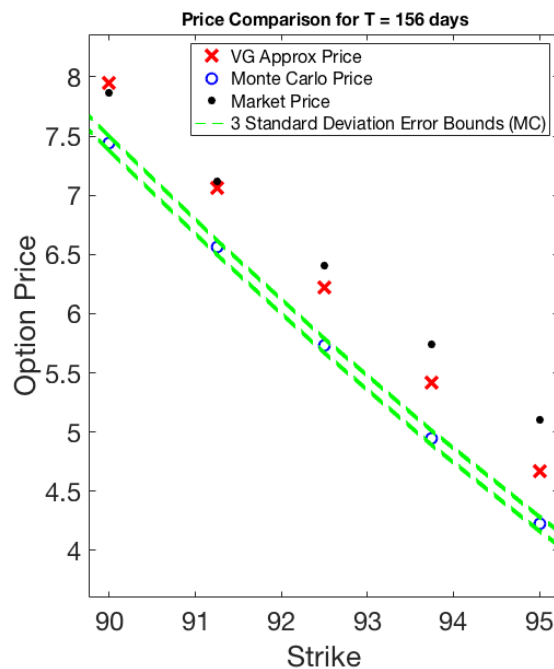


Fig. 7.5: The zoomed in price comparison for the call option on the KBW Index on 16 January 2019 with maturity of 156 days (grey circle from Figure 7.4)

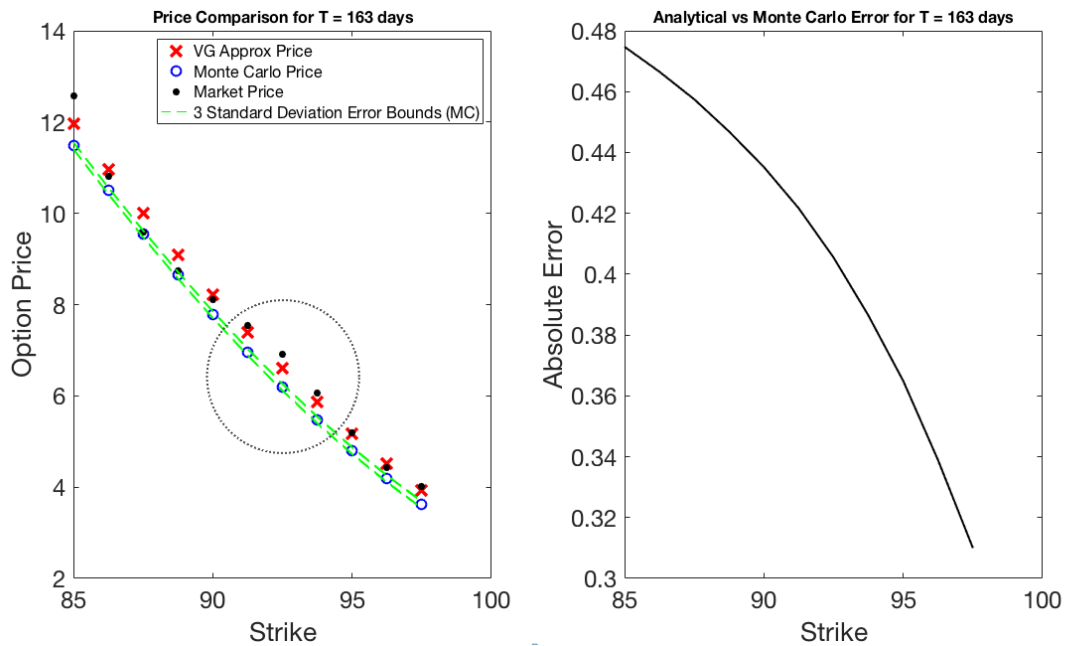


Fig. 7.6: A price comparison of Monte Carlo prices (circles), analytical approximation prices (crosses) and market prices (dots), for a call option on the KBW Bank Index on 16 January 2019 with maturity of 163 days

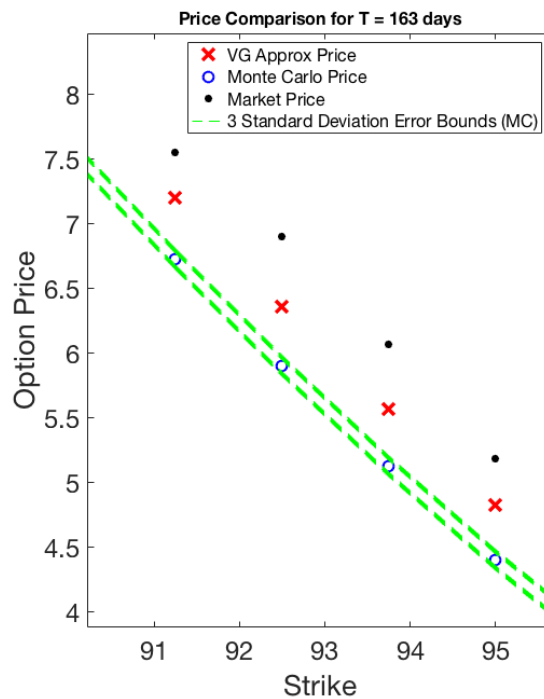


Fig. 7.7: The zoomed in price comparison for the call option on the KBW Index on 16 January 2019 with maturity of 163 days (grey circle from Figure 7.6)

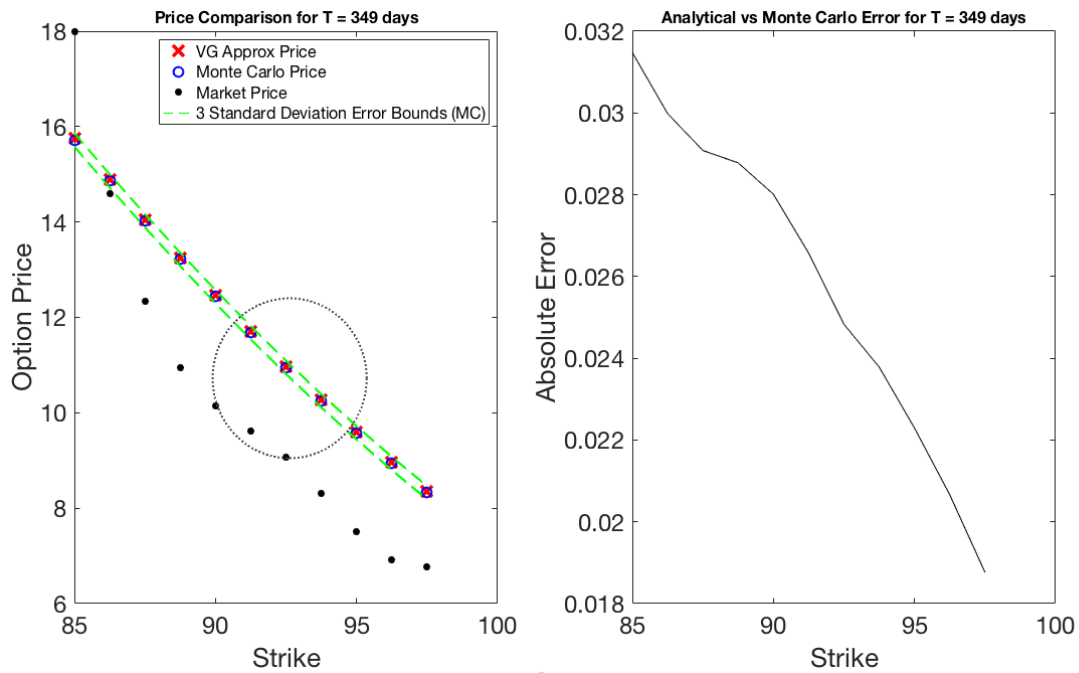


Fig. 7.8: A price comparison of Monte Carlo prices (circles), analytical approximation prices (crosses) and market prices (dots), for a call option on the KBW Bank Index on 16 January 2019 with maturity of 349 days

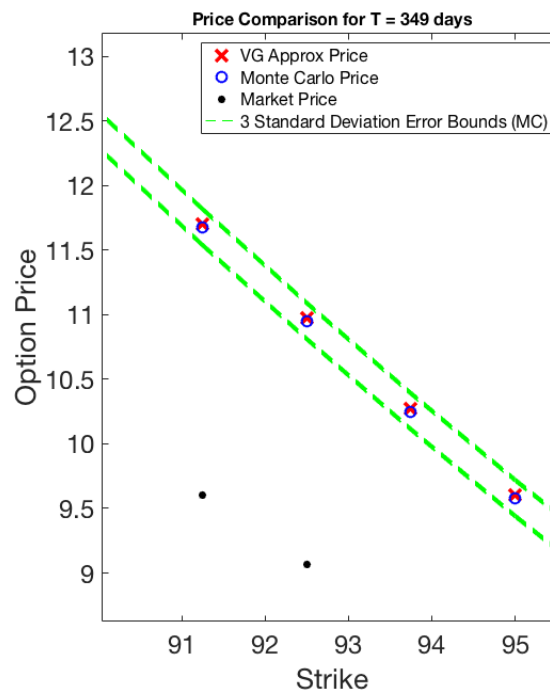


Fig. 7.9: The zoomed in price comparison for the call option on the KBW Index on 16 January 2019 with maturity of 349 days (grey circle from Figure 7.8)

Tab. 7.5: The analytical approximation prices vs the Monte Carlo prices for a basket call option on 16 January 2019

Time to Maturity (days)	Strike	Analytical Price	Monte Carlo Price	Absolute Error	RMSE
156	85.00	11.88	11.33	0.549	0.493
	86.25	10.85	10.31	0.541	
	87.50	9.85	9.32	0.534	
	88.75	8.88	8.36	0.525	
	90.00	7.95	7.44	0.516	
	91.25	7.06	6.56	0.505	
	92.50	6.22	5.73	0.490	
	93.75	5.42	4.95	0.472	
	95.00	4.67	4.22	0.449	
	96.25	3.98	3.55	0.423	
97.50	3.34	2.95	0.391		
163	85.00	11.97	11.46	0.516	0.463
	86.25	10.95	10.44	0.508	
	87.50	9.96	9.46	0.501	
	88.75	9.00	8.51	0.493	
	90.00	8.08	7.60	0.483	
	91.25	7.20	6.73	0.473	
	92.50	6.36	5.90	0.460	
	93.75	5.57	5.13	0.444	
	95.00	4.83	4.40	0.425	
	96.25	4.14	3.74	0.400	
97.50	3.50	3.13	0.370		
349	85.00	15.75	15.72	0.031	0.026
	86.25	14.89	14.86	0.030	
	87.50	14.06	14.03	0.029	
	88.75	13.25	13.22	0.029	
	90.00	12.46	12.43	0.028	
	91.25	11.71	11.68	0.027	
	92.50	10.98	10.95	0.025	
	93.75	10.28	10.25	0.024	
	95.00	9.60	9.58	0.022	
	96.25	8.96	8.94	0.021	
97.50	8.34	8.32	0.019		

7.2.2 Multivariate Normal Inverse Gaussian Model

The multivariate NIG model was used in the analytical approximation and Monte Carlo prices shown in Figures 7.10 - 7.15. Figures 7.11, 7.13 and 7.15 are the zoomed-in versions of Figures 7.10, 7.12 and 7.14, respectively. The grey dotted-lined circle in Figures 7.10, 7.12 and 7.14 shows the area that is zoomed-in and displayed in Figures 7.11, 7.13 and 7.15. This is done to illustrate the Monte Carlo error bounds more clearly, as the standard deviation of the Monte Carlo prices is very small and difficult to see in all of the figures.

If we analyse the results for the 156 and 163 day maturities in Figures 7.10 - 7.13, we notice that the fit of the analytical approximation to the Monte Carlo is very similar, just as it was for the multivariate VG model prices. We note this is due to the fact that these two maturities differ only by one week. Comparing the RMSEs, the RMSE for the 156 day maturity results is 0.538 and for the 163 day maturity results is 0.533. Figures 7.10 - 7.13 illustrate the fit of the analytical results to the Monte Carlo prices, and we observe, once again, that the results for both 156 and 163 day maturities do not fit the Monte Carlo within the three standard deviation error bounds. However, the absolute error graphs for these two maturities show the opposite trend to that found in the multivariate VG model - the absolute error between the analytical approximation prices and the Monte Carlo prices initially increases with increasing strike, until it passes the at-the-money strike (94.89), where it starts to decrease again.

The results for the 349 day maturity show that the analytical approximation produces the best results in terms of the convergence to Monte Carlo prices. This trend was also observed for the multivariate VG model in section 7.2.1. Figure 7.9 shows how the analytical approximation prices fit within the standard deviation error bounds and sit very closely to the Monte Carlo circles. Table 7.8 details the absolute errors and it is shown that the highest absolute error is only 0.081, which is lower than the lowest absolute error for both the 156 and 163 day maturities. This suggests that the analytical approximation, once again, performs better for longer-dated maturities, in terms of fit to the Monte Carlo prices. It is also evident that the absolute errors also tend to decrease as the strikes increase, the same trend that was found for the results of all the maturities in section 7.2.1, where the multivariate VG model was implemented - see Figure 7.14.

Tab. 7.6: A Summary of the RMSE and absolute errors between the Monte Carlo and analytical approximation prices for basket options with various maturities, when implemented for the multivariate NIG model

Error	Days to Maturity		
	156 day	163 day	349 day
RMSE	0.538	0.533	0.073
Highest absolute error	0.607	0.591	0.081
Lowest absolute error	0.421	0.434	0.061

For both the multivariate VG and multivariate NIG models, we notice the general trend is the same, whereby we observe that the convergence of the analytical approximation prices to the Monte Carlo prices improves as the length of time to maturity increases. With regards to the multivariate NIG model, we see that the analytical approximation falls out of these error bounds for options that have shorter expiries (i.e. 156 and 163 days) whereas the 349 day maturity option prices fit well within the error bounds. This was the same observation made for the multivariate VG model. If we analyse the numbers presented in Table 7.6, we see that the RMSE, which is based on 11 options, is smallest for the 349 day expiry (RMSE = 0.073) and largest for the shortest expiry at 156 day RMSE = 0.538. The RMSE for the 163 day maturity is not far from the 156 day RMSE, at 0.533, but motivates the observation that the analytical prices converge more accurately to the Monte Carlo prices for longer maturities. As with the multivariate VG model prices, the trend is also illustrated in Table 7.6 by the highest and lowest relative errors between the analytical approximation and the Monte Carlo price, for the different maturities. For more detailed prices, see Table 7.8. The evidence presented in section 7.2.1 and the current section alludes to the fact that the analytical approximation performs better for longer-dated maturities, in pricing basket options, for both the exponential Lévy models.

However, when we compare the multivariate VG model of section 7.2.1 with the multivariate NIG model, we find that although the analytical approximation results present consistent trends in terms of length of time to maturity, the analytical approximation produces slightly better results for the multivariate VG model, as these results show better convergence to Monte Carlo prices. We can see this by comparison of the RMSE values for the various maturities and both models, which is shown for clarity in Table 7.7 below. We see that the multivariate VG model prices outperform those of the multivariate NIG model prices, for all the maturities. The 349 day maturity results show the lowest RMSE for both models, but the multivari-

ate VG model has a RMSE of 0.026, in comparison to the RMSE of the multivariate NIG model, which is 0.073. In contrast, the highest RMSE value is for the 156 day maturity results for both the models, but sits at 0.493 for the multivariate VG model and a slightly higher 0.538 for the multivariate NIG model.

Tab. 7.7: A comparison of the RMSE values between the Monte Carlo and analytical approximation prices for basket options with various maturities, for the multivariate VG model versus the multivariate NIG model

RMSE	Days to Maturity		
	156 day	163 day	349 day
Multivariate VG Model	0.493	0.463	0.026
Multivariate NIG Model	0.538	0.533	0.073

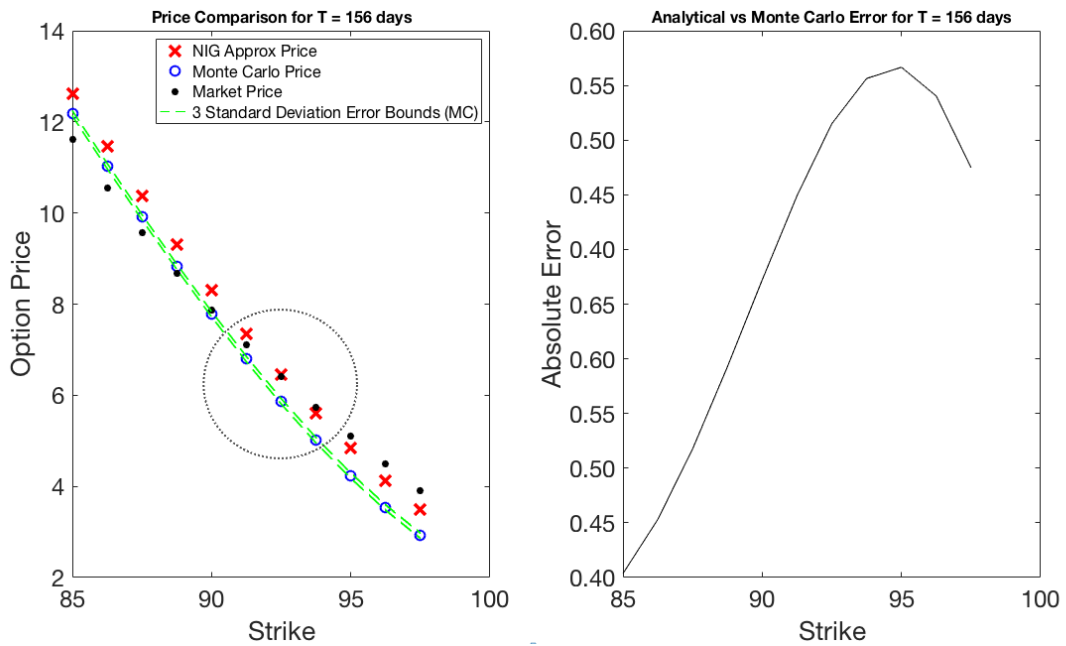


Fig. 7.10: A price comparison of Monte Carlo prices (circles), analytical approximation prices (crosses) and market prices (dots), for a call option on the KBW Bank Index on 16 January 2019 with maturity of 156 days

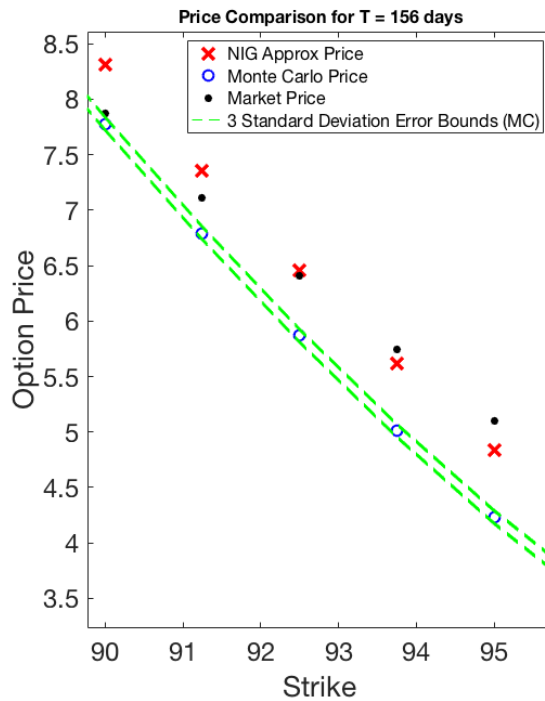


Fig. 7.11: The zoomed in price comparison for the call option on the KBW Index on 16 January 2019 with maturity of 156 days (Grey circle from Figure 7.10)

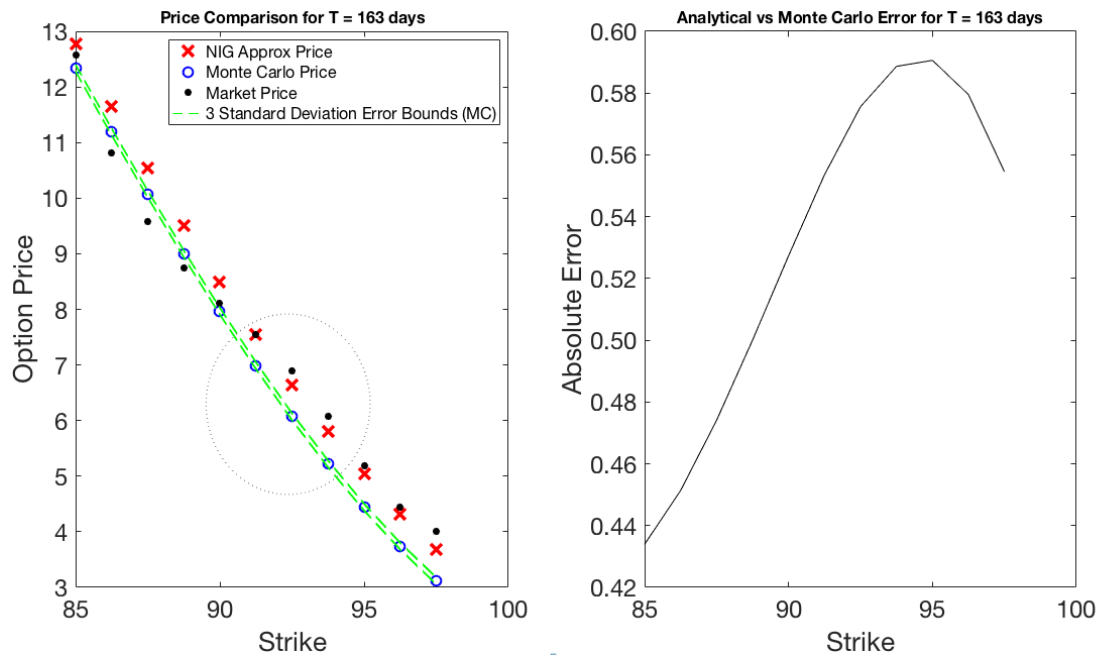


Fig. 7.12: A price comparison of Monte Carlo prices (circles), analytical approximation prices (crosses) and market prices (dots), for a call option on the KBW Bank Index on 16 January 2019 with maturity of 163 days

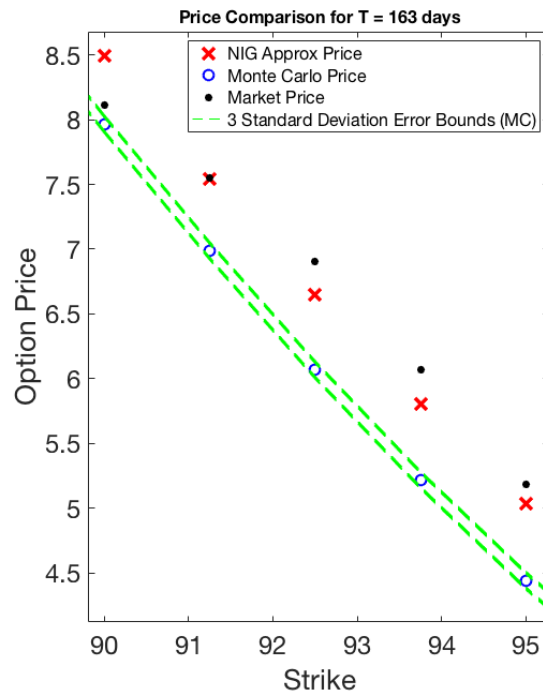


Fig. 7.13: The zoomed in price comparison for the call option on the KBW Index on 16 January 2019 with maturity of 163 days (Grey circle from Figure 7.12)

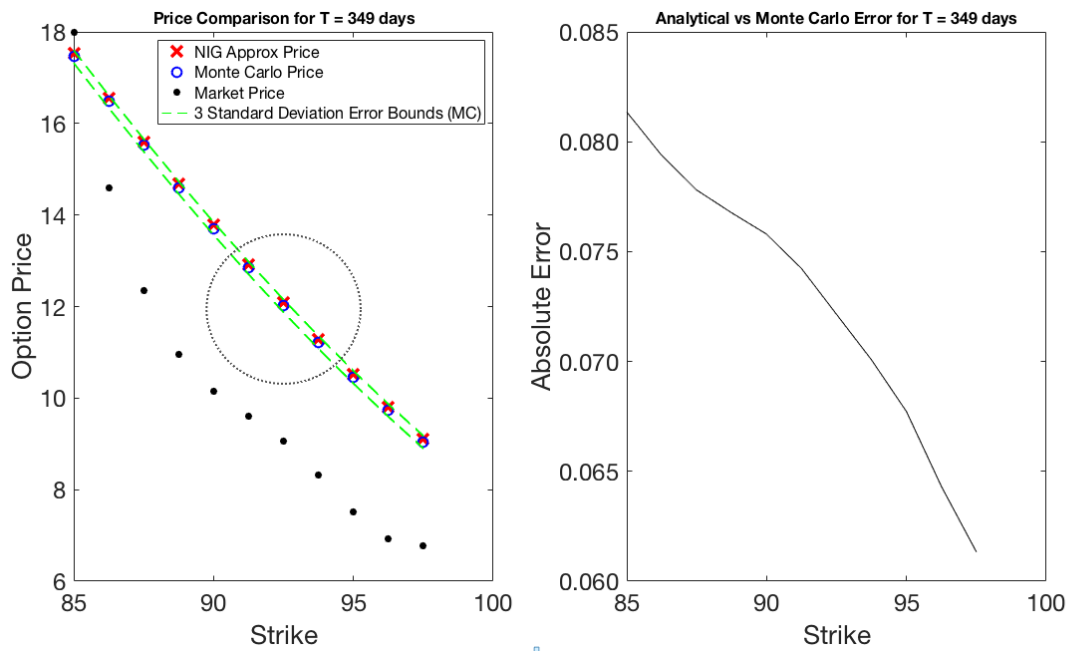


Fig. 7.14: A price comparison of Monte Carlo prices (circles), analytical approximation prices (crosses) and market prices (dots), for a call option on the KBW Bank Index on 16 January 2019 with maturity of 349 days

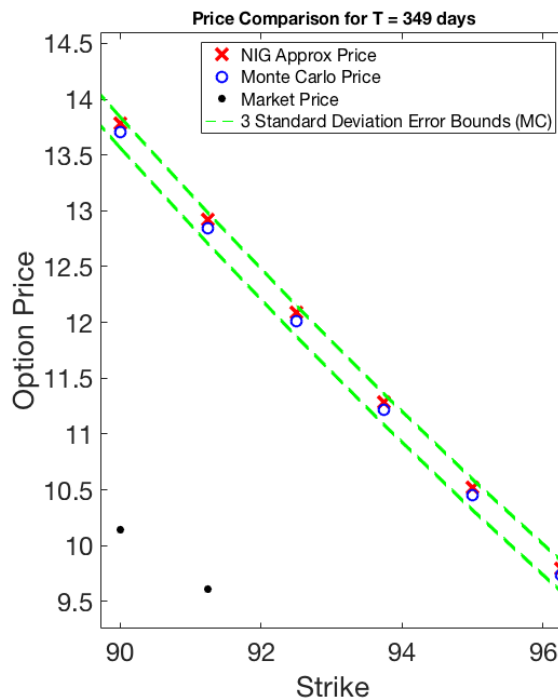


Fig. 7.15: The zoomed in price comparison for the call option on the KBW Index on 16 January 2019 with maturity of 349 days (Grey circle from Figure 7.14)

Tab. 7.8: The analytical approximation prices vs the Monte Carlo prices for a basket call option on 16 January 2019

Time to Maturity (days)	Strike	Analytical Price	Monte Carlo Price	Absolute Error	RMSE
156	85.00	12.61	12.19	0.421	0.538
	86.25	11.47	11.03	0.441	
	87.50	10.37	9.91	0.467	
	88.75	9.32	8.82	0.497	
	90.00	8.31	7.78	0.529	
	91.25	7.35	6.79	0.560	
	92.50	6.45	5.87	0.586	
	93.75	5.62	5.01	0.602	
	95.00	4.84	4.23	0.607	
	96.25	4.13	3.54	0.596	
97.50	3.49	2.92	0.570		
163	85.00	12.77	12.34	0.434	0.533
	86.25	11.64	11.19	0.451	
	87.50	10.55	10.08	0.474	
	88.75	9.50	9.00	0.500	
	90.00	8.49	7.97	0.527	
	91.25	7.54	6.99	0.554	
	92.50	6.65	6.07	0.576	
	93.75	5.81	5.22	0.589	
	95.00	5.03	4.44	0.591	
	96.25	4.32	3.74	0.580	
97.50	3.67	3.12	0.555		
349	85.00	17.54	17.46	0.081	0.073
	86.25	16.56	16.48	0.079	
	87.50	15.60	15.52	0.078	
	88.75	14.68	14.60	0.077	
	90.00	13.78	13.70	0.076	
	91.25	12.92	12.84	0.074	
	92.50	12.09	12.01	0.072	
	93.75	11.29	11.22	0.070	
	95.00	10.52	10.46	0.068	
	96.25	9.80	9.73	0.064	
97.50	9.10	9.04	0.061		

In terms of efficiency, (measured by how long it takes for the code on Matlab to execute), the Monte Carlo is significantly faster for both 100 000 and 1 million simulations. As is shown in Table 7.9, the Monte Carlo process has an execution time of approximately 0.4 seconds for 100 000 simulations and the analytical approximation takes 250 times longer at around 100 seconds, thus the analytical approximation does not compete with the Monte Carlo in terms of efficiency.

Tab. 7.9: A comparison of the efficiency of the pricing methods, in terms of the run-time of the code

Pricing Method	Run Time of Code (in seconds)		
	156 day	163 day	349 day
Analytical Approximation	100.48	97.29	99.56
Monte Carlo (100 000 simulations)	0.40	0.37	0.36
Monte Carlo (1 000 000 simulations)	3.88	4.12	4.07

The Monte Carlo with 1 million simulations is approximately 10 times slower than the Monte Carlo with 100 000 simulations, as is expected. The analytical approximation is a lot less efficient than the Monte Carlo method. A deeper analysis into the code execution time (using the Matlab profiler) showed that approximately 90.6% of the execution time was being used by the `fsolve` function (which is a function that is used to solve nonlinear equations), which was needed to solve both Equations 4.18 and 4.28.

Chapter 8

Conclusion

This dissertation explored the use of exponential Lévy models to price basket options. The motivation was driven by the increasing interest in multi-asset products in the financial market, and thus the search for models that are able to better fit real market data. The two exponential Lévy models that were used were the multivariate VG and the multivariate NIG model. The models were calibrated to univariate options data from the market using the non-linear least squares method. Both models were able to accurately fit vanilla options on the KBW Bank Index constituents, as measured by the relatively small root mean square errors between the model and market prices. A basket option based on the KBW Bank Index was then priced using the Monte Carlo pricing method as well as an analytical approximation method (as derived by [Linders and Stassen \(2016\)](#)). The analytical approximation, originally developed for the multivariate VG model, was extended to allow for use of the multivariate NIG model. It was found that the analytical approximation provided an accurate expression for the price of a basket option, by means of a Monte Carlo simulation study, using both multivariate VG and NIG models. A comparison of the models was carried out using the Monte Carlo pricing method and real market data. It was established that the multivariate NIG model outperformed that of the multivariate VG model for pricing options of shorter maturity, in that it was able to match market prices with more accuracy than the multivariate VG model. However, for longer-dated maturities, it was found that the multivariate VG model actually outperformed the multivariate NIG model. Another comparison was drawn between the two models, where the analytical approximation was implemented and measured against the Monte Carlo prices. We discovered that the general trend was that, as the length of time to maturity of the options increased, so too did the convergence of the analytical approximation prices to the Monte Carlo method. Both models displayed this trend, however the multivariate VG model was able to outperform the multivariate NIG model slightly, in terms of convergence. In terms of efficiency, we see that the Monte Carlo method is 250

times faster than the approximation, in terms of the execution time of the code. All things considered, the analytical approximation formula for the exponential Lévy models still provide an accurate fit to real market data, as well as Monte Carlo pricing, with the multivariate VG model coming out as superior to the multivariate NIG model in terms of pricing basket options.

Bibliography

- Avramidis, A. N. and L'Ecuyer, P. (2006), 'Efficient Monte Carlo and quasi-Monte Carlo option pricing under the Variance Gamma model', *Management Science* **52**(12), 1930–1944.
- Ballotta, L. and Bonfiglioli, E. (2016), 'Multivariate asset models using Lévy processes and applications', *The European Journal of Finance* **22**(13), 1320–1350.
- Barndorff-Nielsen, O. E. (1997), 'Normal inverse gaussian distributions and stochastic volatility modelling', *Scandinavian Journal of statistics* **24**(1), 1–13.
- Barndorff-Nielsen, O. E., Mikosch, T. and Resnick, S. I. (2012), *Lévy processes: theory and applications*, Springer Science & Business Media.
- Benth, F. E., Groth, M. and Kettler, P. C. (2006), 'A quasi-Monte Carlo algorithm for the normal inverse Gaussian distribution and valuation of financial derivatives', *International Journal of Theoretical and Applied Finance* **9**(06), 843–867.
- Benth, F. E. and Šaltytė-Benth, J. (2004), 'The normal inverse gaussian distribution and spot price modelling in energy markets', *International journal of theoretical and applied finance* **7**(02), 177–192.
- Boyle, P., Broadie, M. and Glasserman, P. (1997), 'Monte Carlo methods for security pricing', *Journal of economic dynamics and control* **21**(8-9), 1267–1321.
- Carr, P., Geman, H., Madan, D. B. and Yor, M. (2003), 'Stochastic volatility for Lévy processes', *Mathematical Finance* **13**(3), 345–382.
- Carr, P. and Wu, L. (2004), 'Time-changed Lévy processes and option pricing', *Journal of Financial Economics* **71**(1), 113–141.
- Chen, J. (2018), 'KBW Bank Index', <https://www.investopedia.com/terms/k/kbw-bank-index.asp>.
- Cont, R. and Tankov, P. (2003), *Financial modelling with jump processes*, Vol. 2, CRC press.
- Dhaene, J., Denuit, M., Goovaerts, M. J., Kaas, R. and Vyncke, D. (2002), 'The concept of comonotonicity in actuarial science and finance: theory', *Insurance: Mathematics and Economics* **31**(1), 3–33.

- Folks, J. L. and Chhikara, R. S. (1978), 'The inverse gaussian distribution and its statistical applications a review', *Journal of the Royal Statistical Society: Series B (Methodological)* **40**(3), 263–275.
- Hirsa, A. and Madan, D. B. (2004), 'Pricing American options under Variance Gamma', *Journal of Computational Finance* **7**(2), 63–80.
- Kaas, R., Goovaerts, M., Dhaene, J. and Denuit, M. (2008), *Modern actuarial risk theory: using R*, Vol. 128, Springer Science & Business Media.
- Kalemanova, A., Schmid, B., Werner, R. et al. (2007), 'The normal inverse Gaussian distribution for synthetic CDO pricing', *Journal of derivatives* **14**(3), 80.
- Kyprianou, A. E. (2006), *Introductory lectures on fluctuations of Lévy processes with applications*, Springer Science & Business Media.
- Kyprianou, A., Schoutens, W. and Wilmott, P. (2006), *Exotic option pricing and advanced Lévy models*, John Wiley & Sons.
- Linders, D. and Stassen, B. (2016), 'The multivariate Variance Gamma model: basket option pricing and calibration', *Quantitative Finance* **16**(4), 555–572.
- Luciano, E., Marena, M. and Semeraro, P. (2016), 'Dependence calibration and portfolio fit with factor-based subordinators', *Quantitative Finance* **16**(7), 1037–1052.
- Luciano, E. and Schoutens, W. (2006), 'A multivariate jump-driven financial asset model', *Quantitative finance* **6**(5), 385–402.
- Madan, D. B., Carr, P. P. and Chang, E. C. (1998), 'The Variance Gamma process and option pricing', *Review of Finance* **2**(1), 79–105.
- Madan, D. B. and Seneta, E. (1987), 'Chebyshev polynomial approximations and characteristic function estimation', *Journal of the Royal Statistical Society. Series B (Methodological)* pp. 163–169.
- Madan, D. B. and Seneta, E. (1990), 'The Variance Gamma (VG) model for share market returns', *Journal of business* pp. 511–524.
- Nasdaq (2018), 'KBW Nasdaq Bank Index Methodology', https://indexes.nasdaqomx.com/docs/Methodology_BKX.pdf.
- Papapantoleon, A. (2008), 'An introduction to Lévy processes with applications in finance', *arXiv preprint arXiv:0804.0482*.
- Rathgeber, A. W., Stadler, J. and Stöckl, S. (2016), 'Modeling share returns-an empirical study on the Variance Gamma model', *Journal of Economics and Finance* **40**(4), 653–682.
- Sæbø, K. K. (2009), Pricing Exotic Options with the normal inverse Gaussian market model using numerical path integration, Master's thesis, Institutt for matematiske fag.

- Sato, K.-i. (1999), *Lévy processes and infinitely divisible distributions*, Cambridge University Press.
- Schoutens, W. (2002), *The Meixner process: theory and applications in finance*, Eindhoven University of Technology.
- Schoutens, W. (2003), *Lévy processes in finance*, Wiley.
- Semeraro, P. (2008), 'A multivariate Variance Gamma model for financial applications', *International journal of theoretical and applied finance* **11**(01), 1–18.
- Sheikh, A. Z. and Qiao, H. (2010), 'Non-normality of market returns: A framework for asset allocation decision making', *The Journal of Alternative Investments* **12**(3), 8.
- Tweedie, M. (1941), 'A mathematical investigation of some electrophoretic measurements on colloids', *M. Sc. Thesis, University of Reading*.
- Wu, Y.-C., Liao, S.-L. and Shyu, S.-D. (2009), 'Closed-form valuations of basket options using a multivariate normal inverse gaussian model', *Insurance: Mathematics and Economics* **44**(1), 95–102.

Appendix A

Variance of the Price of the Basket

As is expressed in Equation 4.4, the basket is a weighted sum of stocks.

The covariance of the Brownian motions can be denoted as follows:

$$\text{cov}(\vec{B}) = \mathbb{E}[\vec{B} \vec{B}^T] = CC^T = \rho$$

where ρ is the correlation matrix.

and C is the Cholesky decomposition, which can be written as a matrix $(C_{ij})_{ij}$, such that:

$$B_t^i = \sum_k C_{ik} W_t^k$$

where W^k are independent one-dimensional standard Brownian motions.

By expanding equation 4.5, the following is obtained:

$$S = a_1 e^{b_1 + \mu_1 y + \sigma_1 \sqrt{y} B_1} + a_2 e^{b_2 + \mu_2 y + \sigma_2 \sqrt{y} B_2} + \dots + a_n e^{b_n + \mu_n y + \sigma_n \sqrt{y} B_n}$$

where:

$$a_i = w_i X_i(0) ; b_i = (r - q_i + \omega_i)T$$

The variance of S is obtained as follows:

$$\begin{aligned} \text{Var}(S) &= \text{Cov}(S, S) \\ &= \text{Cov}\left(a_i e^{b_i + \mu_i y + \sigma_i \sqrt{y} B_i}, a_j e^{b_j + \mu_j y + \sigma_j \sqrt{y} B_j}\right) \\ &= A_{ij}(y) \text{Cov}\left(e^{\sigma_i \sqrt{y} B_T^i}, e^{\sigma_j \sqrt{y} B_T^j}\right) \end{aligned}$$

where:

$$A_{ij} := a_i a_j e^{(b_i + b_j) + (\mu_i + \mu_j)y}$$

Now:

$$\begin{aligned} \text{Cov} \left(e^{\sigma_i \sqrt{y} B_T^i}, e^{\sigma_j \sqrt{y} B_T^j} \right) &= \mathbb{E} \left[e^{\sigma_i \sqrt{y} B_T^i + \sigma_j \sqrt{y} B_T^j} \right] - \mathbb{E} \left[e^{\sigma_i \sqrt{y} B_T^i} \right] \mathbb{E} \left[e^{\sigma_j \sqrt{y} B_T^j} \right] \\ &= \mathbb{E} \left[e^{\sigma_i \sqrt{y} \sum_k C_{ik} W_T^k + \sigma_j \sqrt{y} \sum_k C_{jk} W_T^k} \right] - e^{\frac{1}{2} \sigma_i^2 y T} e^{\frac{1}{2} \sigma_j^2 y T} \\ &= \prod_k \mathbb{E} \left[e^{(\sigma_i C_{ik} + \sigma_j C_{jk}) \sqrt{y} W_T^k} \right] - e^{\frac{1}{2} (\sigma_i^2 + \sigma_j^2) y T} \end{aligned}$$

by independence of W_T^k

$$\begin{aligned} &= \prod_k e^{-\frac{1}{2} (\sigma_i C_{ik} + \sigma_j C_{jk})^2 y T} - e^{\frac{1}{2} (\sigma_i^2 + \sigma_j^2) y T} \\ &= e^{\frac{1}{2} \sum_k (\sigma_i C_{ik} + \sigma_j C_{jk})^2 y T} - e^{\frac{1}{2} (\sigma_i^2 + \sigma_j^2) y T} \end{aligned}$$

Hence,

$$\text{Cov} \left(a_i e^{b_i + \mu_i y + \sigma_i \sqrt{y} B_T^i}, a_j e^{b_j + \mu_j y + \sigma_j \sqrt{y} B_T^j} \right) = a_i a_j e^{(b_i + b_j) + (\mu_i + \mu_j) y} \left(e^{\frac{1}{2} \sum_k (\sigma_i C_{ik} + \sigma_j C_{jk})^2 y T} - e^{\frac{1}{2} (\sigma_i^2 + \sigma_j^2) y T} \right)$$

In particular, with $i = j$, we obtain:

$$\begin{aligned} \text{Var} \left(a_i e^{b_i + \mu_i y + \sigma_i \sqrt{y} B_T^i} \right) &= a_i^2 e^{2(b_i + \mu_i y)} \left(e^{2 \sum_k \sigma_i^2 C_{ik}^2 y T} - e^{\sigma_i^2 y T} \right) \\ &= a_i^2 e^{2(b_i + \mu_i y)} \left(e^{2 \sigma_i^2 y T} - e^{\sigma_i^2 y T} \right) \end{aligned}$$

Since

$$\sum_k C_{ik}^2 = (CC^T)_{ii} = \rho_{ii} = 1$$

Then,

$$\text{Var}(S) = \sum_{ij} \text{Cov} \left(a_i e^{b_i + \mu_i y + \sigma_i \sqrt{y} B_T^i}, a_j e^{b_j + \mu_j y + \sigma_j \sqrt{y} B_T^j} \right)$$